APTD-0981

PB 210 671

ELECTRONICS LABORATORY • SYRACUSE, N.Y.

Final Report:

FIELD STUDY ON APPLICATION OF LASER COINCIDENCE ABSORPTION MEASUREMENT TECHNIQUES

February 1972

Contract EHSD 71-8

Prepared for

ENVIRONMENTAL PROTECTION AGENCY

Durham, North Carolina 27701

GENERAL ELECTRIC

Reproduced by
NATIONAL TECHNICAL
INFORMATION SERVICE
U.S. Department of Commerce
Springfield VA 22151

U.S.

15

BIBLIOGRAPHIC DATA SHEET	1. Report No. APTD-0981	2.	3. Recipient's Accession No.
4. Title and Subtitle: Field Study on Application of Laser Coincidence Absorption Measurement Techniques			5. Report Date: February 1972 6.
7. Author(s)			8. Performing Organization Rept. No.
9. Performing Organization Name and Address: General Electric Electronics Laboratory Syracuse, New York			10. Project/Task/Work Unit No. 11. Contract/Grant No. EHSD 71-8
12. Sponsoring Organization Name and Address: ENVIRONMENTAL PROTECTION AGENCY Durham, North Carolina 27701			13. Type of Report & Period Covered: Final 14.

15. Supplementary Notes

16. Abstracts: The purpose was to conduct a field study on the merits and limitations of laser coincidence absorption measurement technique applied to long-path monitoring of a gaseous pollutant in an urban atmosphere. Two gaseous pollutants, ethylene and ammonia, were selected and spectral interferences identified. Laser wavelengths were selected and appropriate weighting functions calculated and read into the signal processor. Using a spectrally tunable CO_2 laser, measurements and system evaluation were conducted at Cazenovia, New York. This rural test site was used to calibrate the system and conduct measurements under variable conditions of weather, time of day, temperature, etc. A site was selected in Syracuse, New York which provided a good average sampling of the pollutant gases. The laser system was moved to this location. Measurements made at the rural test site were repeated under similar conditions of time and weather. Selected pollutant concentrations and spectral interference effects were recorded. Concurrent point measurements were made by gas chromatograph for ethylene concentrations. Overall system effectiveness and test results were analyzed and performance evaluated.

17. Key Words and Document Analysis. 17a. Descriptors

Air Pollution
Lasers
Field tests
Ethylene
Ammonia
Rural areas
Urban areas

17b. Identifiers/Open-Ended Terms

17c. COSATI Field/Group 13 B

18. Availability Statement	19. Security Class (This Report)	21. No. of Pages
Unlimited	UNCLASSIFIED	75
	20. Security Class (This Page) UNCLASSIFIED	22. Price $4.50

TABLE OF CONTENTS

Section	Title	Page
I	SCOPE	1/2
II	INTRODUCTION AND SUMMARY	1/2
III	DESCRIPTION OF THE LASER SYSTEM	3
	A. INTRODUCTION	3
IV	PRELIMINARY STUDY AND SYSTEM OPTIMIZATION	9
	A. OBJECTIVES	9
	B. SUMMARY OF RESULTS IN PRELIMINARY STUDY	9
	C. AMMONIA SURVEY	9
	D. ETHYLENE SURVEY	13
	E. SELECTION OF SPECTRAL LINES	14
	F. SELECTION OF LINEAR WEIGHTS	27
V	TEST PLAN	29
	A. OBJECTIVE	29
	B. EQUIPMENT	29
	1. Cazenovia Test Site	29
	2. Urban Site	30
	C. MEASUREMENT PROCEDURES	30
	1. Cazenovia	30
	2. Urban Site	33
	D. DATA RECORDING	33
	1. Data Format	33
	2. Ambient Conditions	35
	E. DATA ANALYSIS	36
VI	RURAL TEST SITE MEASUREMENTS PROGRAM	37
	A. SUMMARY OF RURAL TEST RESULTS	37
	B. RURAL TEST SITE	38
	C. RURAL TEST RESULTS	38

TABLE OF CONTENTS
(concluded)

Section	Title	Page
VII	TRANSFER TO URBAN SITE	55
VIII	URBAN TEST SITE MEASUREMENTS PROGRAM	59
	A. SUMMARY OF URBAN TEST RESULTS	59
	B. URBAN TEST RESULTS	59
	C. SYSTEM IMPROVEMENT WITH A CLEANUP APERTURE	65
IX	SUMMARY OF SYSTEM PERFORMANCE EVALUATION . .	67
	1. Severe Scintillation Induced by Local Heat Sources	67
	2. Long Term Unbalance or Drift Error Produced by Changing the Attitude or Pointing Direction of the Laser Transceiver and then Correcting for this by Translating the Germanium Focusing Lens at the Entrance to the Beam Expander . . .	67
	3. Unbalance Caused by Aiming Error from Transmitter to Retroreflector	67
	4. Direct Coupled Amplifier Drift and Paper Slippage in the Chart Recorders	68
	5. Errors Caused by System Noise	68
	6. Unusually Large Scintillation Caused by Defocusing the Retrotelescope	68
	7. Detection of 14 ppb Ethylene, 19 ppb Ammonia . .	69
	8. Projected Performance Capability	69
X	REFERENCES	70

LIST OF ILLUSTRATIONS

Figure No.	Title	Page
1.	ILAMS Block Diagram	4
2.	"V" Laser Optical Layout	5
3.	Four-Wavelength Signal Processing Block Diagram	6
4.	Breadboard System at Rural Site	7/8
5a.	Power Output versus Wavenumber for "V" Laser Using a Mode-limiting Circular Mode Stop	16
5b.	Power Output versus Wavenumber for "V" Laser Using a Mode-limiting Circular Mode Stop	17
6.	Transmission Spectrum of Ethylene	18
7.	Transmission Spectrum of Ammonia	19
8.	Transmission Spectrum of Ozone	20
9.	Transmission Spectrum of an Automobile Exhaust Sample Automotive Exhaust - Cold Idle - 10 Meter Cell	21
10.	Atmospheric Transmission over a 0.3 km Path in the Chesapeake Bay area	22
11.	Carbon Dioxide Absorption and Water Vapor Absorption in Solar Spectra	23
12.	Measured 10.59μ Transmittance of Water Vapor in Air at 23^{o}C versus the Partial Pressure of Water Vapor for a 980-m Path	24
13.	The Logarithms of the 9.55μ and 10.59μ Transmittance of Water Vapor at 25^{o}C versus Pressure for a 980-m Path	25
14.	Rural Test Facility Profile	39
15.	Photo of Cazenovia Valley	39
16.	ILAMS Transceiver and Recording Equipment at Rural Test Site	40
17.	27-foot Gas Cell at Rural Test Site	40
18.	Contours of Equal Power Density at the Beam Expander Output	42
19.	Chart Record	51/52
20.	Relationship Between Scintillation and Weather at Rural Site	53
21.	Relationship Between Scintillation and Noise and Drift	54
22.	Urban Test Site Photos	57

LIST OF ILLUSTRATIONS (concluded)

Figure No.	Title	Page
23.	Relationship Between Scintillation and Weather at Urban Site (Skytop)	63
24.	Relationship Between Scintillation and Noise and Drift (Urban Site)	64
26.	Location of Cleanup Aperture	66

LIST OF TABLES

Table No.	Title	Page
I.	SUMMARY OF ETHYLENE SURVEY IN SYRACUSE, N. Y.	10
II.	RESULTS OF AMMONIA MONITORING BY THE ONONDAGA COUNTY HEALTH DEPARTMENT IN 1969	12
III.	AMMONIA SOURCES IN SYRACUSE, NEW YORK -- COUNTY EMISSION SURVEY FOR 1969	13
IV.	POWER OUTPUT VERSUS WAVELENGTH AND WAVE NUMBER FOR THE CO_2 LASER SYSTEM	17
V.	10.59μ WATER VAPOR AND CO_2 EXTINCTION COEFFICIENTS AND LOSS PER KILOMETER AT 25^{o}C (77^{o}F)	24
VI.	RELATIVE SYSTEM RESPONSE ASSUMING TWO WAVE-LENGTHS	25
VII.	MEASURED ABSORPTION COEFFICIENTS	27
VIII.	SETS OF OPTIMUM LINEAR WEIGHTS	28
IX.	STANDARD DATA RECORDING SHEET	34
X.	LAST 24 HOURS OF DATA TAKEN AT RURAL TEST SITE IN CAZENOVIA, N. Y.	49/50
XI.	URBAN TEST SITE DATA	62

I. SCOPE

The purpose of this program is to conduct a field study on the merits and limitations of laser coincidence absorption measurement technique applied to long-path monitoring of a gaseous pollutant in an urban atmosphere.

II. INTRODUCTION AND SUMMARY

The program was conducted in five phases:

Preliminary Study and System Optimization - During this phase, two gaseous pollutants, ethylene and ammonia, were selected and spectral interferences identified. Laser wavelengths were selected and appropriate weighting functions calculated and read into the signal processor. The phase objective was to optimize system sensitivity to the selected gases while rejecting spectral interference effects.

Rural Test Site Measurements - Using GE's spectrally tunable CO_2 laser, measurements and system evaluation were conducted at Cazenovia, New York. This rural test site was used to calibrate the system and conduct measurements under variable conditions of weather, time of day, temperature, etc.

Transfer to Urban Test Site - With EPA approval, a site was selected in Syracuse, New York which provided a good average sampling of the pollutant gases. The laser system was moved to this location.

Urban Test Site Measurements - Measurements made at the rural test site were repeated under similar conditions of time and weather. Selected pollutant concentrations and spectral interference effects were recorded. Concurrent point measurements were made by gas chromatograph for ethylene concentrations.

System Performance Evaluation - Overall system effectiveness and test results were analyzed and performance evaluated. The conclusions are summarized in this report.

III. DESCRIPTION OF THE LASER SYSTEM

A. INTRODUCTION

In order to understand the meaning of this measurements program, it is necessary to understand the system. The laser system used in this program is a breadboard system constructed by the General Electric Company under an internally funded program. The system operates in the middle region of the infrared spectrum and identifies atmospheric constituents by absorption spectroscopy. It measures average pollutant concentrations over long ranges at relatively low, safe power levels. ILAMS (Infrared Laser Atmospheric Monitoring System) consists of a spectrally scanning laser, transmit-receive optics, a signal processor and a retroreflector. The system transmits energy at four wavelengths in a rapid sequence to a remote retroreflector located (depending upon the operational situation) from one to ten or more miles away. This laser function is called spectral scanning.

Laser power densities are kept below safety limits by expanding the beam 0.5 watt (5×10^{-3} watts/cm^2) at the laser and 0.015 watts (2×10^{5} watts/cm^2) at the retroreflector. Energy returned from the retroreflector is collected in a collinear transmit-receive optical system and referenced to laser output energy to compensate for power differences at each wavelength. Energy attenuation at the selected lasing wavelengths produces a pattern of absorption versus wavelength with which the system identifies pollutants and registers their average concentration over the path (double the laser to retroreflector distance) traversed by the beam.

An ILAMS block diagram is shown in Figure 1. The output power from the laser is directed to a 50-percent beamsplitter. The energy transmitted through the beamsplitter is focused down to a 0.004-inch aperture that serves as an attenuator for the detector and as a simulator for the retroreflector. Behind this aperture is the reference energy detector. The energy at this focal point of the output beam has the same energy distribution in cross-section as does the far-field pattern of the laser, but on a smaller scale. Any changes in the energy distribution in the far-field due to laser noise will have the same effect on the reference detector as it does on the energy collected by the retroreflector. Because of diffraction, the energy that passes through the aperture spreads out in a 5-degree cone. A thermistor bolometer detector behind the aperture picks up the central part of this cone and the attenuation is varied by controlling the aperture to bolometer spacing.

The reflected power from the beamsplitter goes through a germanium lens which focuses the energy near the focal point of an off-axis parabolic mirror. The energy then reflects off a 45-degree flat mirror to the parabola, and the expanded, nearly collimated beam is transmitted to the retroreflector. The

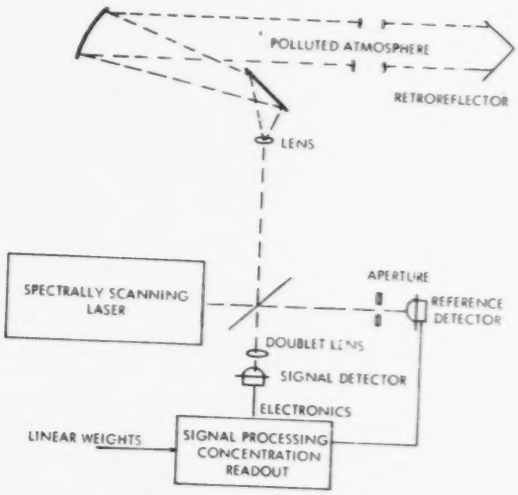

Figure 1. ILAMS Block Diagram

return energy from the retroreflector retraces the path through the beam-expanding parabolic mirror and the germanium lens to the beamsplitter. The energy reflected from the beamsplitter is lost, but that which is transmitted is collected by a germanium lens doublet and focused on the signal detector. Preamplifiers are mounted directly behind the signal and reference detectors; the preamp outputs go to the signal processor. The detectors used in the system are thermistor bolometers operating at ambient temperature (uncooled) and giving a characteristic flat response across the middle infrared spectral region.

The attenuation of laser energy at many wavelengths produces absorption patterns enabling the system's signal processor to effectively separate pollutant effects from spectral interferences. To aid in the selection of these wavelengths, off-line computer programs have been developed using inputs such as the available number of lasing lines, their wavelengths and power, the number of pollutants, interferences and spectral data. The computer sorts through the data produced, to rank wavelength combinations according to their effectiveness in pollutant discrimination. Linear weights for use in the system's signal processor are calculated with efficient computer programs developed for this purpose. The weights are manually set into the system's signal processor. Returned signals at each of the lasing wavelengths are weighted and summed by the processor to cancel interference effects and produce pollutant concentration readouts.

The CO_2 laser in the breadboard system is alignable to four wavelengths. These wavelengths may be selected from the more than 70 available with $C^{12}O_2^{16}$. The laser is presently designed to detect ethylene and ammonia in a spectral environment that is expected to contain neutral attenuation, ozone, water vapor, and gasoline engine exhaust fumes and a random spectral attenuator such as atmospheric scintillation might produce. The wavelengths selected were 9.505, 10.532, 10.675 and 10.719 microns.

The optical configuration of the laser is shown in Figure 2. The term "V-laser" comes from the shape of the plasma tube. A relatively long laser cavity is used for sufficient gain to overcome the losses inherent in the spectral tuner and to obtain lasing action on a large number of spectral lines. A beam travels through the plasma tube with aid of a mirror at the point of the V. Leaving the tube through a germanium Brewster window, the beam is directed by mirrors through an iris (for mode control) and onto a 105 lines/mm diffraction grating having a dispersion of 105 mr/micron which disperses the beam spectrally and spatially. The four wavelengths of interest are then relayed (intercepted) first by two mirrors, and after passing through holes in the chopper wheel, by the four end mirrors of the laser cavity. These holes are so located that, as the wheel turns, only one wavelength at a time is permitted to pass through to the end mirrors. The four end or wavelength selection mirrors are adjusted so that the beams are directed back on themselves and through the laser cavity. In this way, selected laser wavelengths are transmitted sequentially at a rapid rate. A typical chopping wheel speed, 4800 rpm, sends all four wavelengths out in 1/80th of a second.

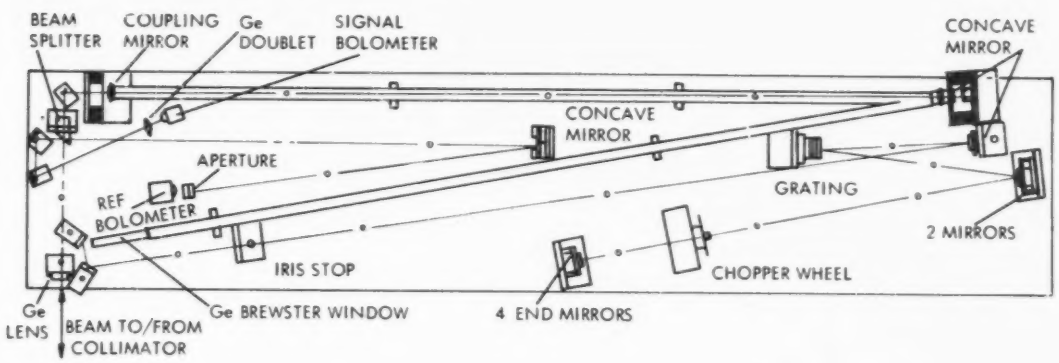

Figure 2. "V" Laser Optical Layout

A block diagram for the four-channel (four wavelength) signal processor is shown in Figure 3. The design is general and can be expanded to accommodate more wavelengths by duplication of the circuits following the log amplifier and difference amplifier.

A low-noise preamplifier having a low frequency voltage gain of 2,000 increases the detector signal to a usable level. High-frequency compensation in the preamplifier corrects for the 1.3 millisecond response time of the bolometer. The frequency response of the two together is flat out to 3,000 Hz with a 3-dB break at 7,500 Hz.

The AGC amplifier, "A", is required to provide a constant average output with variations of return signal strength. This AGC is desirable in order to stay within the optimum dynamic range of the log amplifier. AGC amplifier "B" is required to compensate for the average effects of AGC amplifier "A", as well as to correct for gain changes in the reference energy channel.

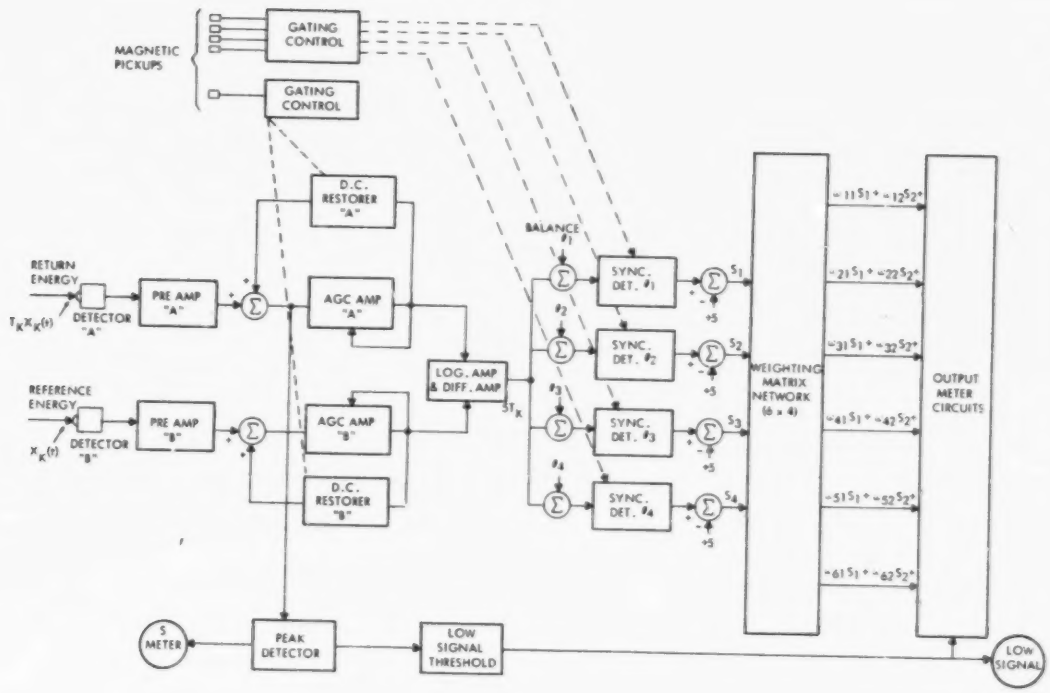

Figure 3. Four-Wavelength Signal Processing Block Diagram

The function of the d-c restorer is to set the d-c zero level of the signal after it passes through the a-c coupled preamplifier. Sampling and controlling the d-c level of the AGC output provides offset compensation and a convenient sensing point for AGC control. A peak detector and meter provide a visual indication of the return signal level. A low-signal threshold presents a visual indication if the signal drops below a preset level.

After the log of the ratio of the return energy to the reference energy is obtained at the output of the difference amplifier, the transmission information is extracted by synchronous detectors gated in synchronism with the laser wavelength scanning. Each synchronous detector is balanced to zero by an added voltage to compensate for any fixed spectral attenuation. An absorption in any channel is detected as a calibrated d-c voltage which is indicated on the signal meters.

The balanced synchronous detector outputs are weighted and summed. The resultant d-c voltage is indicated on the output meters, each of which represents an absorber or class of absorbers. The gating control circuits translate information from the magnetic pickups on the chopper wheel into timing signals which control the operation of the synchronous detectors and the d-c restorers.

Breadboard transmit-receive optics expand the laser beam to a diameter of 5 inches which reduces transmitted power densities to values below 0.01 watt per square centimeter while also contributing to beam collimation. The "cat's eye" style retroreflector is a 12-inch-diameter f/4 parabolic mirror with a 48-inch focal length and a one-inch-diameter, 40-inch-radius-of-curvature, concave, spherical mirror at its focal point. The resolution of the retroreflector is sufficient to return 90% of the incident laser energy to the receiver at one-mile range. Such operational characteristics give the system an operating range of 10 miles or more under conditions of "good visibility".

Figure 4 shows the present unit at the rural test site. While satisfactory for current feasibility studies, these are breadboard components, with substantial reduction in size possible. The V laser is mounted on an aluminum channel, 6 feet in length. Repackaging the present analog functions will afford a considerable reduction in size of the signal processing electronics. Breadboard electronic components, excluding meters and substituting fixed resistors and trimpots for weighting potentiometers could be packaged in a volume of about 2 × 4 inches. According to our studies, digital signal processing, (cost effective when the number of transmitted wavelengths exceeds six) would not have an adverse effect on processor size. A 10 × 40 inch laser breadboard having comparable performance characteristics has also been developed by us under a separate program.

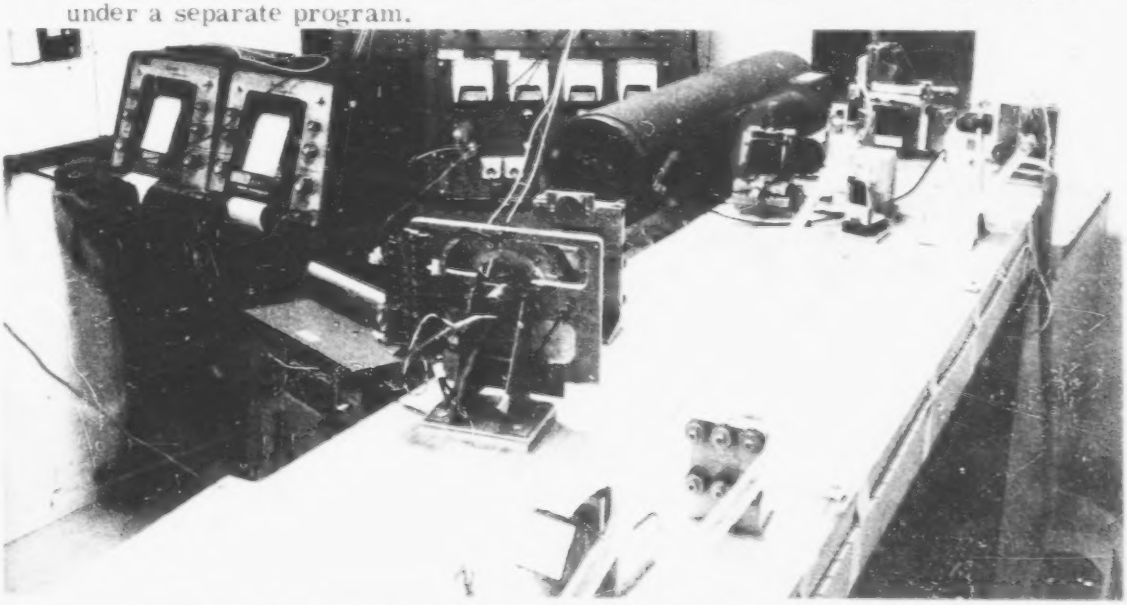

Figure 4. Breadboard System at Rural Site

IV. PRELIMINARY STUDY AND SYSTEM OPTIMIZATION

A. OBJECTIVES

The goals of this preliminary portion of the program are to select a pollutant and determine the significant spectral interferences from pollution monitoring data and laboratory analysis of atmospheric samples. Using this information, the system is adjusted to optimize its sensitivity to the selected pollutant gas while rejecting the effects of spectral interferences.

B. SUMMARY OF RESULTS IN PRELIMINARY STUDY

Ammonia measurements made in central Syracuse, New York in 1969 gave measured concentrations ranging from 0.043 parts per million to 0.148 parts per million. These data are twenty-four hour averages taken every twelve days throughout 1969, and analyzed by NAPCA in Cincinatti.

Ethylene measurements, made by point sampling with a Saran sample bag at downtown locations in Syracuse, gave detectable concentrations of ethylene (5 ppb) about fifty percent of the time. The maximum concentration measured in the open air was 125 ppb at ground level (see Table I.).

Four spectral lines were selected for the detection of both ethylene and ammonia and the laser was aligned to those wavelengths. They are: 10.719 microns (P-32), 10.675 microns (P-28), 10.532 microns (P-14) in the $00^{0}1$-$10^{0}0$ transition and 9.505 microns (P-14) in the $00^{0}1$-$02^{0}0$ transition.

Direct measurements were made of the absorption coefficients of ethylene and ammonia, using the laser as the source. These data were used to determine weighting functions that were set into the signal processor.

C. AMMONIA SURVEY

The data on the concentrations of ammonia in the city of Syracuse, New York were taken from the results of ammonia monitoring by the Onondaga County Health Department in 1969. These data are from twenty-four hour bubbler samples taken from a window in the Water Department building in central Syracuse approximately once every twelve days. The data were analyzed by NAPCA in Cincinatti and the results are presented in Table II.

Table III lists the ammonia sources in Syracuse, New York based on the Onondaga County emission survey for 1969.

TABLE I

SUMMARY OF ETHYLENE SURVEY IN SYRACUSE, N.Y.

DATE	LOCATION	ETHYLENE, CONCENTRATION
12/1/70	637 N. Salina Street downtown at street level; heavy traffic	50 ppb
12/1/70	Corner Water and Salina Streets downtown-street level-heavy traffic	125 ppb
12/1/70	Under Route 81 skyway near Medical Center-heavy traffic	54 ppb
12/23/70	Top floor (5) of Warren Street Parking Garage, 10:30 a.m.	27 ppb
12/24/70	Cazenovia Samples. Two samples collected at test site in country.	0
12/29/70	Inside of Sibleys' parking garage	460 ppb
12/29/70	On top of Sibleys' parking garage in cold cross-wind.	0
1/05/71	Inside of Sibleys' parking garage, no cars	5 ppb (minimum detectable level)
1/05/71	On top of Sibleys' parking garage	0
1/05/71	Erie Blvd. East in Holiday Bowl Parking lot	5 ppb
1/05/71	Corner Teal Avenue and Erie Blvd.	13 ppb
1/11/71	Two samples in East Syracuse Freight Yards	0

(Continued on next page.)

TABLE I (concluded)

SUMMARY OF ETHYLENE SURVEY IN SYRACUSE, N.Y.

DATE	LOCATION	ETHYLENE, CONCENTRATION
1/13/71	Syracuse Airport Runway Sample during use	5 ppb
1/20/71	Three more samples collected around perimeter of airport	0
2/16/71	Four Samples taken at street level on Hiawatha Blvd. near end of lake	0
9/3/71	Two Samples. One at Skytop near laser site, another in Oakwood cemetary on hill top	0
9/9/71	Oakwood Cemetary hill top and Colvin Ave. near gym	0
10/5/71	Top of Sibleys' parking garage	0
10/5/71	Street level at Jefferson	
12/22/71	Men's dormitory at Syracuse University	0

TABLE II

RESULTS OF AMMONIA MONITORING BY THE ONONDAGA COUNTY HEALTH DEPARTMENT IN 1969

DATE	AMMONIA PPM
01/7	0.052
01/19	0.057
01/31	0.063
02/16	0.066
03/08	0.069
03/20	0.073
04/1	0.075
04/13	0.079
04/25	0.058
05/7	0.043
05/19	0.043
05/31	0.076
06/12	0.127
06/24	0.068
07/6	0.086
07/18	0.047
07/30	0.073
08/11	0.043
08/23	0.055
09/4	0.148
09/16	0.063
09/28	0.073
10/10	0.046
10/22	0.062
11/3	0.052

These data are from twenty-four hours bubbler samples taken from a window in the Water Department building once every twelve days.

The above data were received from Bill Compton of Syracuse University Research Corporation on September 25, 1970.

TABLE III

AMMONIA SOURCES IN SYRACUSE, NEW YORK -- COUNTY EMISSION SURVEY FOR 1969

SOURCE	TONS/YEAR	PERCENTAGE OF TOTAL
Industrial Process	193	16.1
Industrial Fuel	719	59.9
Private Fuel	47	3.9
Government Fuel	17	1.4
Commercial Fuel	67	5.6
Refuse Disposal	5	0.4
Transportation	153	12.7

D. ETHYLENE SURVEY

The results of the ethylene survey were presented in Table I. Ambient ethylene was point-monitored by a grab-sample technique. Ten liter samples were pumped into saran bags (from the Anspec Company, Ann Arbor, Michigan) with the aid of a one-liter Hamilton syringe. The sample bags were transported back to the laboratory and analyzed as soon as possible, usually within 30 minutes and always within one hour. Analysis of standard samples by this technique showed no loss of ethylene due to diffusion or wall effects. Quantization was accomplished by use of a Varian-Aerograph Model 1520 gas chromatograph equipped with a flame ionization detector and fitted with a 1/8" × 6' stainless steel column packed with well-aged Chromosorb 102, 60/80 mesh, and operated at 57°C with a nitrogen Carrier gas flow of 50 ml/min. Samples were transferred from the saran bags to the chromatograph by means of 10 ml - Hamilton gas-tight syringes. Calibration curves were constructed using the same type of equipment. The calibration gases were primary standard ethylenes in nitrogen purchased from Matheson.

In earlier experiments, removable sampling loops in a gas sampling valve were packed with an absorbent to trap the ethylene when an air sample was drawn through the loop. Various adsorbents were investigated for this purpose. Calibrated volume vacuum chambers were constructed so that known air volumes might be drawn through the sampling loops in the field without the aid of pumps. The planned procedure was that, once a proper adsorbent was chosen, the instrument could be calibrated and measurements of ethylene levels could begin. Extensive testing of the packed sampling loops for ambient temperature collection of ethylene indicated that the efficiency of adsorption was somewhat lower than expected. This technique was abandoned in favor of the saran bags.

The selection of both Ethylene and Ammonia as pollutants to be monitored by the laser system was based upon two factors:

1) Both pollutants were found to exist in the Syracuse atmosphere in detectable concentrations

2) The four-wavelength GE laser could be aligned to detect both pollutants simultaneously without compromising the system's sensitivity to either one.

E. SELECTION OF SPECTRAL LINES

This laser instrument measures directly the transmission (T_1, T_2, T_3, T_4) of the sample region between the transmitter and the retroreflector at four wavelengths. Assuming that the line width of the resonance absorption is broad compared to the transmitted laser line width, and assuming also that there is no saturation in the absorbing media, then, for a uniform concentration of the absorber over the path, the transmission at each discrete wavelength is of the form, $T_m = \exp(-A_m C_A L)$; where A_m is the absorption coefficient of absorber A at wavelength m, C_A is the concentration of absorber A over the total optical path, and L is the total optical path through the sample region. If the concentration is non-uniform over the path, as is the more usual case, then $C_A L$ can be replaced by the integrated concentration over the path or, more simply, let C_A represent the average concentration over the path.

Typically, C has units of grams/liter or atmospheres of partial pressure, and L is in centimeters. A_m is in units to make $A_m C_A L$ dimensionless.

If a second absorber B with absorption coefficients B_m is introduced into the region, the net transmission will be the product of the transmission due to each absorber.

$$T_m = e^{-[A_m C_A L + B_m C_B L]}$$

If the natural log of the transmission at each wavelength is taken electronically, then

$$\ln T_m = -(A_m C_A L + B_m C_B L)$$

and the resulting signals have two convenient properties:

1) System response to any absorber is a linear function of the quantity (concentration x path) present

2) System response to several absorbers is the sum of the responses to the individual absorbers.

Therefore, if the system can be designed to give a zero response to spectrally interfering absorbers, the system will respond only to the pollutant to be measured, and the response will be proportional to the quantity present.

Using decision theory and multivariate statistical analysis, it can be shown that the optimum signal processing involves the use of single or multiple linear weights. Let $S_1 = -\ln T_1$. Application of a single linear weight, W, means taking a linear sum of the signals S_1, S_2, ... S_n to give a new signal, $S = W_1S_1 + W_2S_2 + \ldots W_nS_n$. The quantity of absorbers present can be accurately determined by examining the magnitude of such linear sums.

Techniques may also be applied for choosing linear weights to accurately measure the quantity of a given pollutant in the presence of known interfering spectral absorbers, random spectral absorbers, scintillation, and other "noises".

On the basis of both analytical and experimental work, several basic conclusions about wavelength selection can be drawn. These are:

1) The relative success of a group of wavelengths depends directly on the measurement problem. The pollutants to be measured, pollutants and absorbers to be ignored, expected quantities of absorbers and the system noise levels, all affect the choice of wavelengths.

2) For a given problem, there will be an optimum set of wavelengths. Increasing the number of pollutants to be estimated or ignored will tend to increase the optimum number of wavelengths to be used; i.e., the more complex the environment, the more wavelengths are necessary.

3) The finer the spectral structure of an absorber, the fewer number of wavelengths are needed to best measure the quantities of it present. The laser system is not limited to detecting pollutants with fine structure such as ammonia and ethylene. In fact, it does remarkably well in detecting or rejecting absorbers with rather smooth spectral characteristics.

4) On the basis of past experience, four wavelengths have done an excellent job in handling spectral recognition problems in environments representative of the real world.

Selection of the best four wavelengths depends upon the relative intensity of the available spectral lines from the laser, the absorption spectra of the target pollutants, the absorption spectra of the other gases and particulate material in the air, and their expected concentrations. The measured spectral lines from the CO_2 laser system in single-mode operation are given in Tables IVa. and IVb. The accompanying Figures (5a. and 5b.) show the same information. Figures 6, 7 and 8 show measured spectra of ethylene, ammonia and ozone, respectively[1]. These data were taken with a single-beam spectrometer having a resolution of 0.1 cm^{-1}. Figure 9 shows a low-resolution spectrum of a typical automobile exhaust fume sample measured with a ten-meter

(1) P. L. Hanst, private communication

TABLE IVa.

POWER OUTPUT VS. WAVELENGTH (AND WAVE NUMBER) FOR THE CO_2 LASER SYSTEM

P	R	Wave Number	Wave Length	Power in Watts	P	R	Wave Number	Wave Length	Power in Watts
J Values					J Values				
38		926.9	10.789	0.24		18	973.2	10.275	0.75
36		928.9	10.765	0.34		20	974.5	10.262	0.74
34		930.9	10.742	0.44		22	976.0	10.248	0.73
32		932.9	10.719	0.50		24	977.0	10.236	0.71
30		934.9	10.696	0.56		26	978.1	10.224	0.65
28		936.8	10.675	0.60		28	979.3	10.211	0.63
26		938.6	10.654	0.63		30	980.6	10.198	0.58
24		940.5	10.633	0.65		32	981.9	10.184	0.52
22		942.3	10.612	0.66		34	983.0	10.173	0.44
20		944.1	10.592	0.66		36	983.8	10.165	0.40
18		945.9	10.572	0.66		38	986.5	10.137	0.15
16		947.7	10.552	0.65		40	987.5	10.126	0.00
14		944.8	10.532	0.64		42	988.6	10.115	0.00
12		951.3	10.512	0.60					
10		953.0	10.493	0.57	42		922.8	10.836	0.04
8		954.6	10.476	0.54	40		924.8	10.812	0.15
6		956.1	10.459	0.40					
4		957.6	10.442	0.00					
2		959.2	10.425	0.00					
	2	961.5	10.400	0.00					
	4	963.0	10.385	0.02					
	6	964.5	10.369	0.40					
	8	965.7	10.355	0.56					
	10	967.2	10.339	0.65					
	12	968.6	10.323	0.70					
	14	970.2	10.307	0.73					
	16	971.9	10.290	0.75					

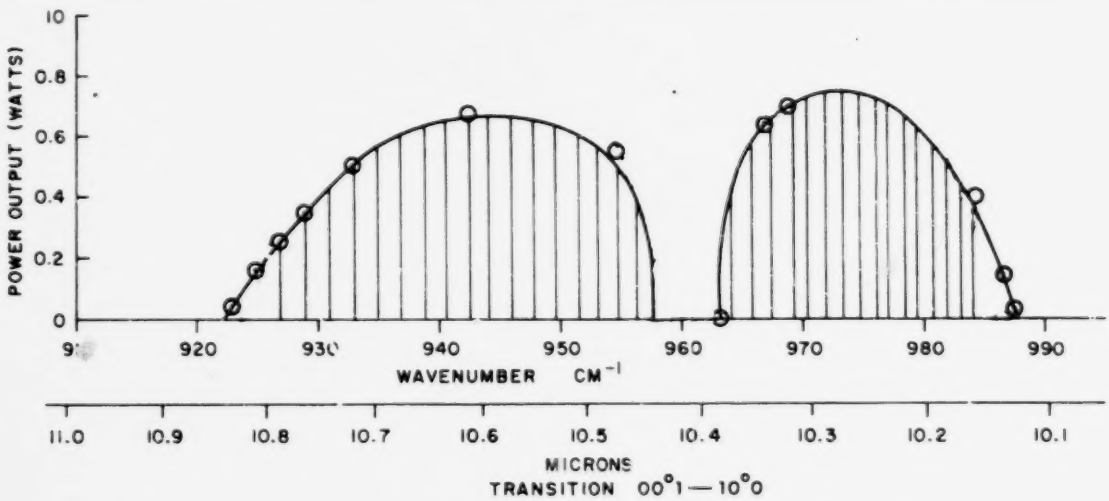

Figure 5a. Power Output vs. Wavenumber for "V" Laser Using a Mode-limiting Circular Mode Stop

TABLE IVb.

POWER OUTPUT VS. WAVELENGTH (AND WAVE NUMBER) FOR THE CO_2 LASER SYSTEM

P J Values	R J Values	Wave Number	Wave Length	Power in Watts	P J Values	R J Values	Wave Number	Wave Length	Power in Watts
38		1029.4	9.714	0.50		18	1075.7	9.296	1.10
36		1031.5	9.694	0.60		20	1077.0	9.285	1.10
34		1033.5	9.676	0.70		22	1078.4	9.273	1.08
32		1035.4	9.658	0.76		24	1079.8	9.262	1.04
30		1037.4	9.639	0.80		26	1081.0	9.251	0.98
28		1039.4	9.621	0.83		28	1082.2	9.240	0.90
26		1041.3	9.603	0.84		30	1083.4	9.230	0.84
24		1043.2	9.586	0.83		32	1084.5	9.221	0.76
22		1045.0	9.569	0.82		34	1086.0	9.201	0.68
20		1046.8	9.553	0.81		36	1087.9	9.192	0.52
18		1048.6	9.537	0.78		38	1088.9	9.188	0.38
16		1050.4	9.521	0.75		40	1090.0	9.174	0.00
14		1052.1	9.505	0.70		42	1090.9	9.166	0.00
12		1053.8	9.489	0.65					
10		1055.6	9.478	0.57	42		1025.2	9.754	0.20
8		1057.4	9.457	0.50	40		1027.4	9.733	0.38
6		1059.1	9.442	0.34					
4		1060.6	9.429	0.02					
2		1062.0	9.416	0.00					
	2	1064.5	9.394	0.00					
	4	1065.8	9.382	0.00					
	6	1067.3	9.369	0.00					
	8	1068.7	9.357	0.50					
	10	1070.1	9.345	0.76					
	12	1071.5	9.333	0.90					
	14	1072.9	9.320	0.98					
	16	1074.3	9.308	1.04					

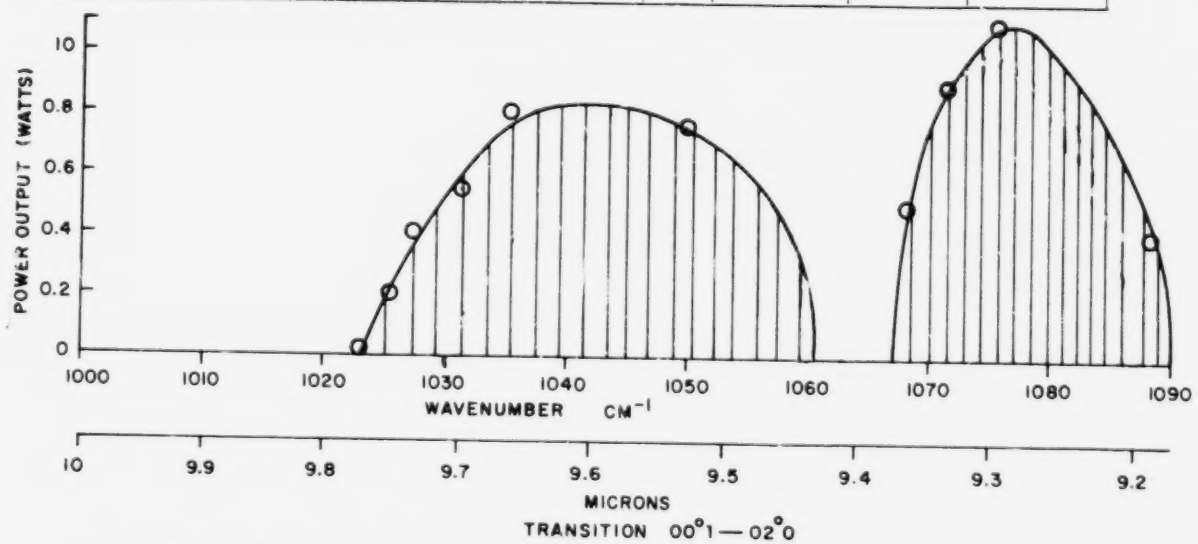

Figure 5b. Power Output vs. Wavenumber for "V" Laser Using a Mode-limiting Circular Mode Stop

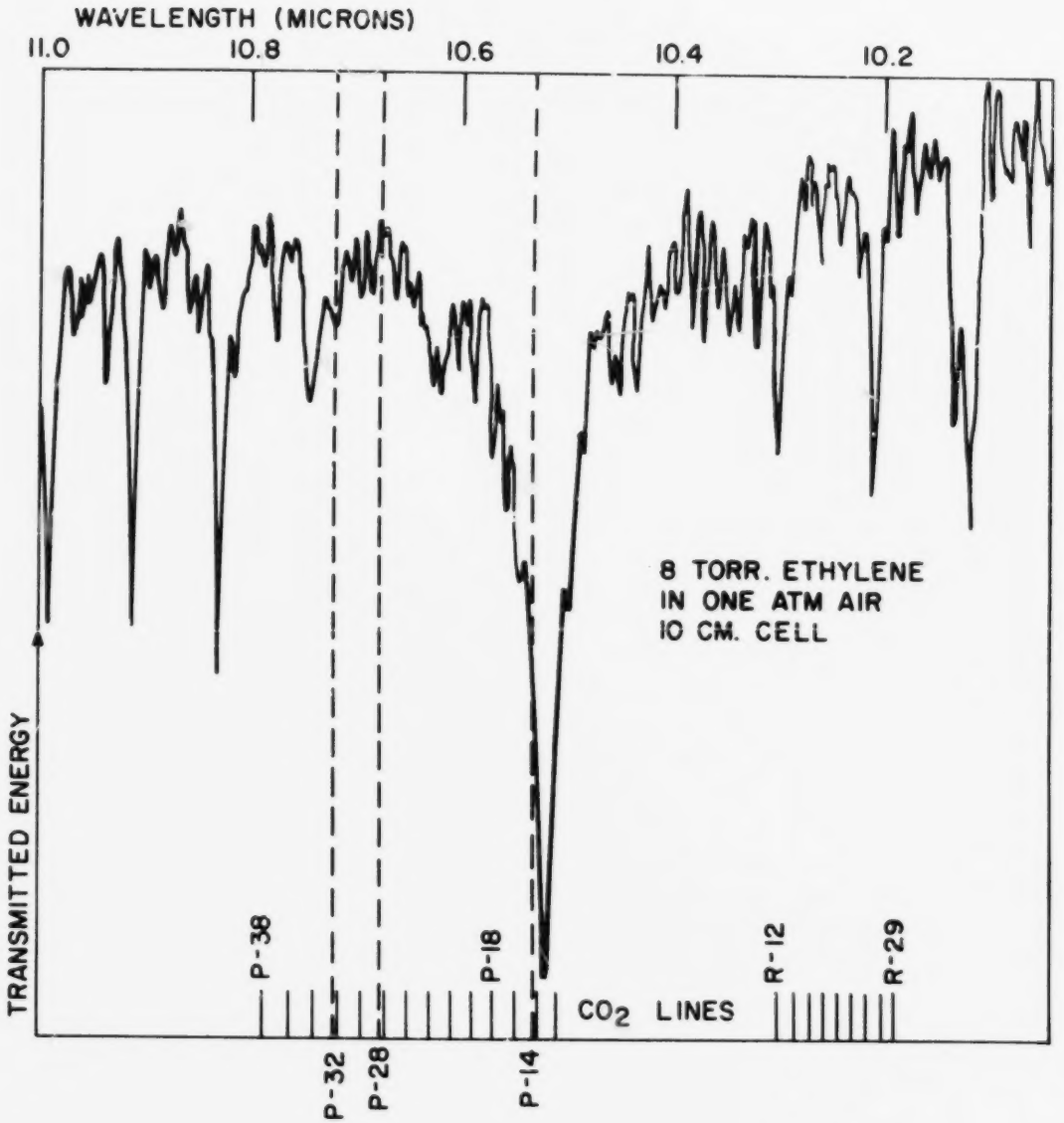

Figure 6. Transmission Spectrum of Ethylene

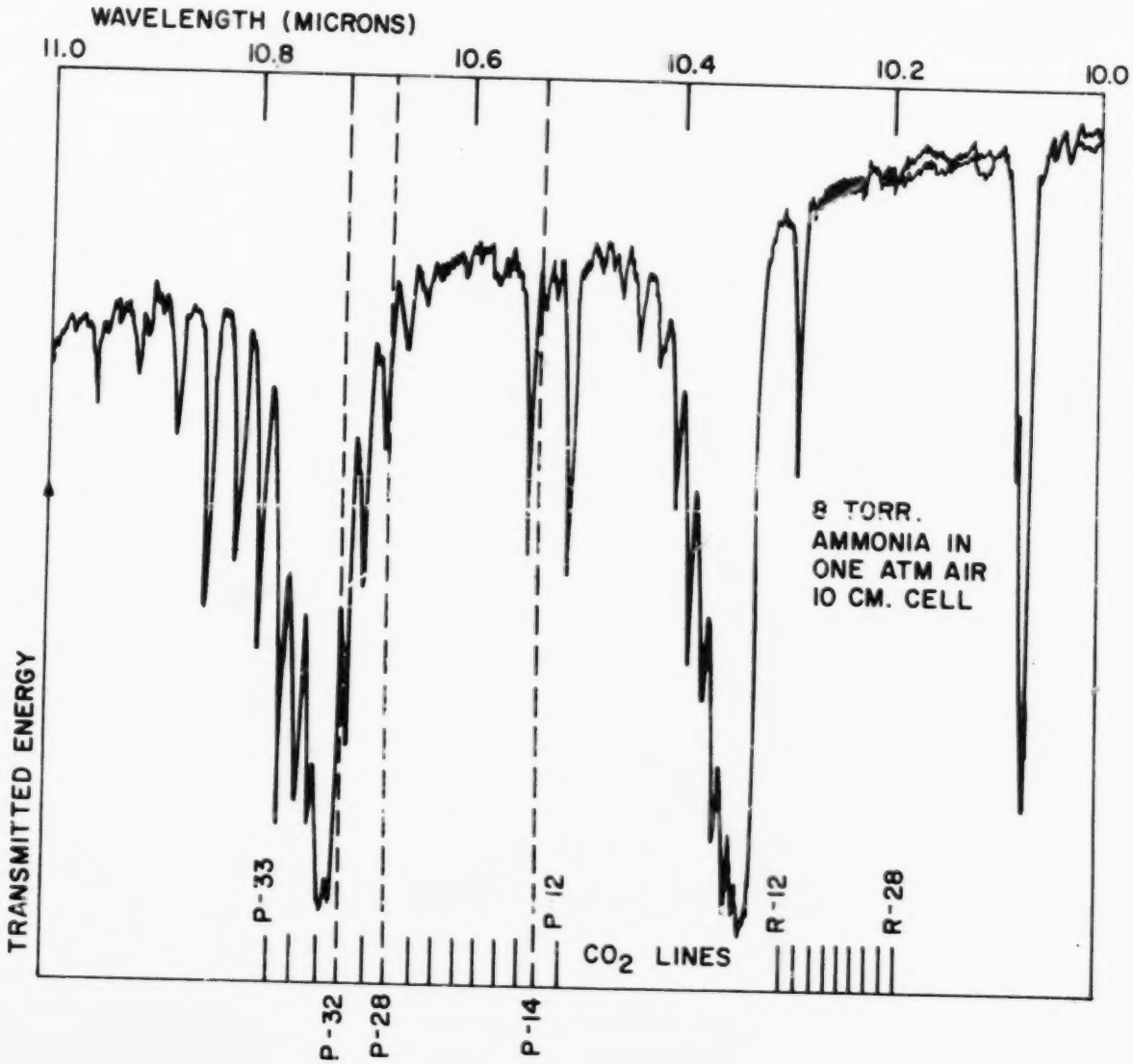

Figure 7. Transmission Spectrum of Ammonia

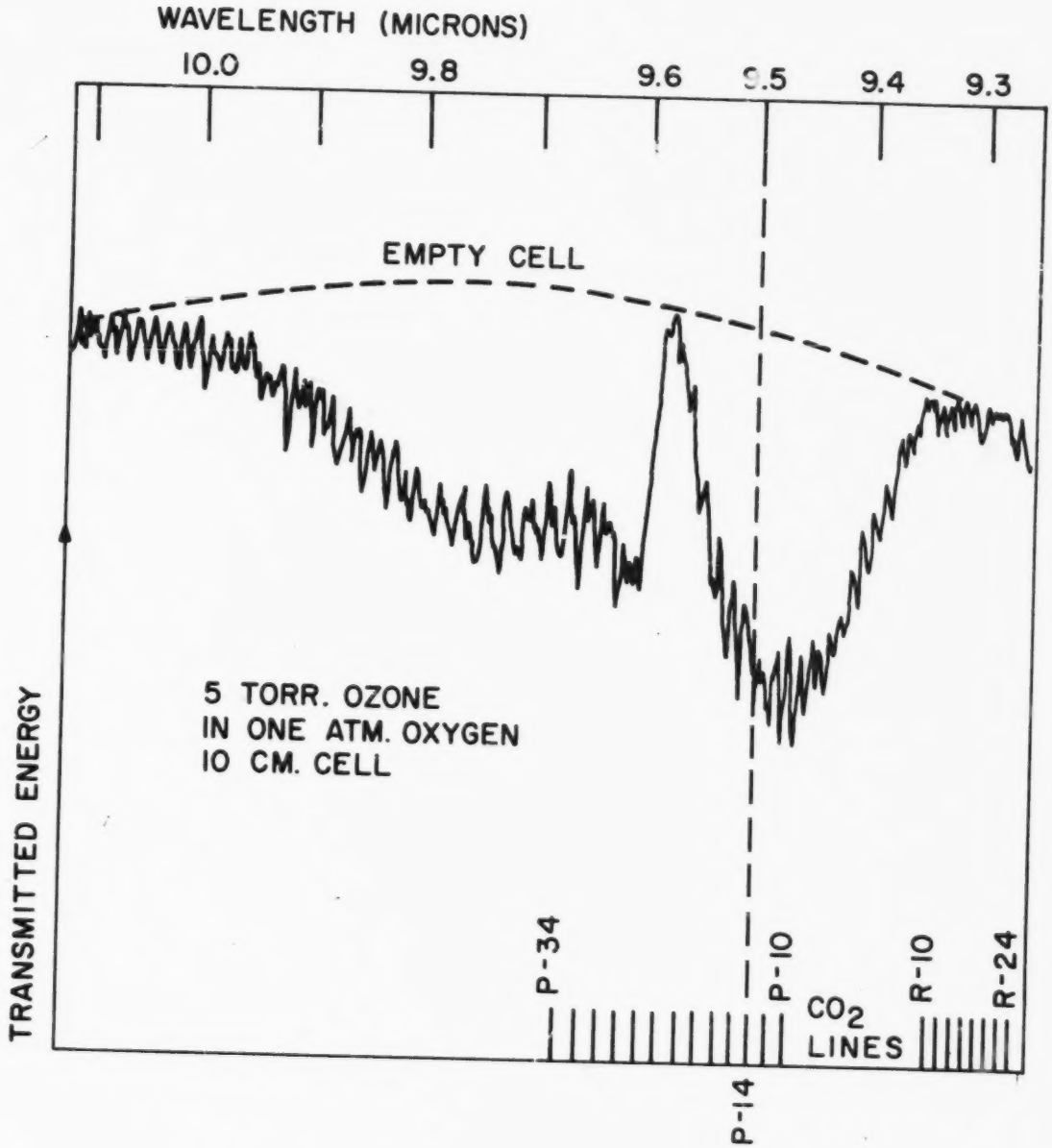

Figure 8. Transmission Spectrum of Ozone

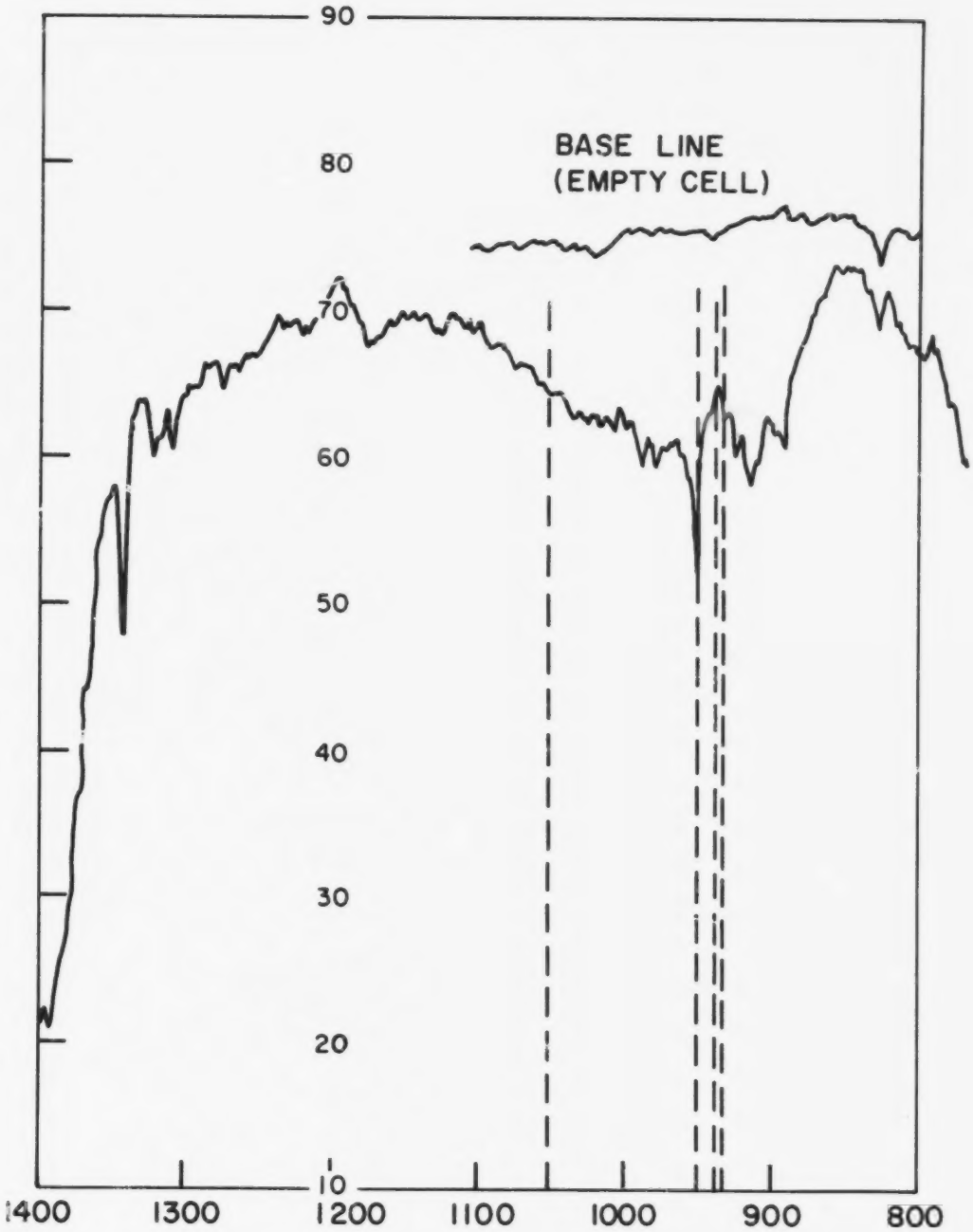

Figure 9. Transmission Spectrum of an Automobile Exhaust Sample
Automotive Exhaust - Cold Idle - 10 Meter Cell

cell on the Beckman IR-9 spectrophotometer. Note that, in Figure 9, the wavelength is increasing from left to right, so that the picture is reversed from that of the other three curves. The selected laser spectral lines are shown on each of these curves. The structure of the absorption pattern for exhaust fumes in all five exhaust samples measured indicates that ethylene is the only significant contributor between 9 and 11 microns. We have concluded that none of the other material in automobile exhaust fumes contributes any significant spectral interference for the CO_2 laser system. The other spectrally interfering materials considered were water vapor and carbon dioxide.

The relation between the CO_2 laser lines and the H_2O absorption line at 10.542 microns is shown in Figures 10 and 11. In Figure 11, the absorption at the line centers is lower and the line widths are larger than would be observed with the laser due to the limiting resolution of the spectrometer; i.e., the profiles shown are instrumental. Note that the P-14 line at 10.532 microns is approximately 0.01 microns (1 cm^{-1}) away from the H_2O line center. The width of the 10.532 micron laser gain line is approximately 0.001 cm^{-1} and the half width of the H_2O absorption line is 0.1 cm^{-1} (see Reference 3).

It may be noted, at this point, that CO_2 in the atmosphere represents a neutral absorption rather than a spectral absorption to the CO_2 laser wavelengths. This is true as long as we restrict the laser to the common isotope of carbon dioxide — $C^{12}O_2^{16}$. The absorption lines are wide compared to the laser gain lines, they have exactly the same centers, and they are of approximately the same strength at the wavelengths where this system will lase.

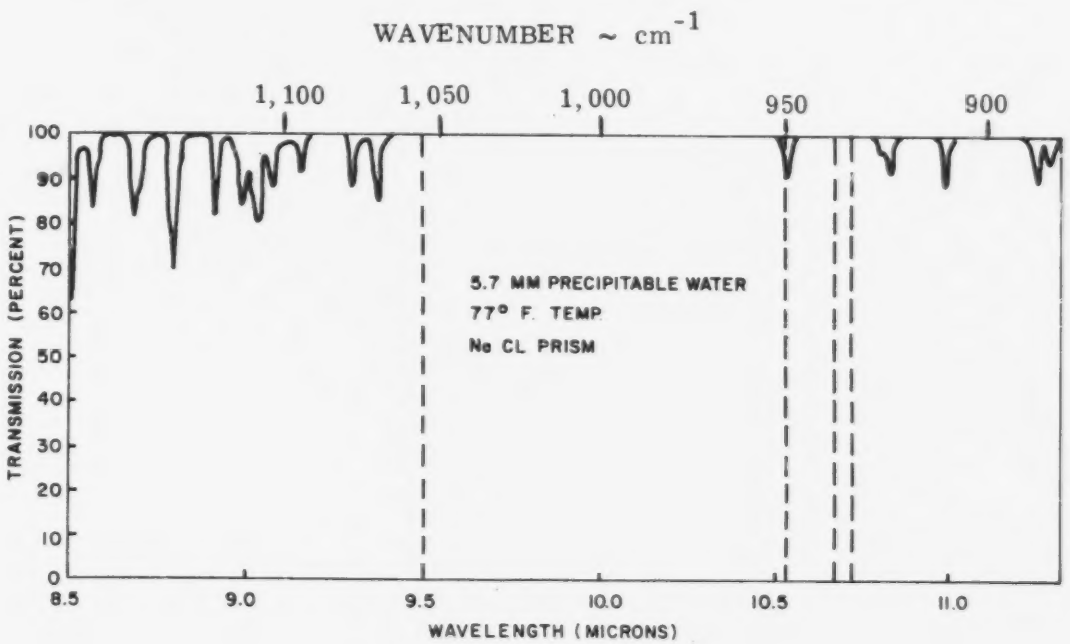

Figure 10. Atmospheric Transmission over a 0.3 km Path in the Chesapeake Bay area [2]

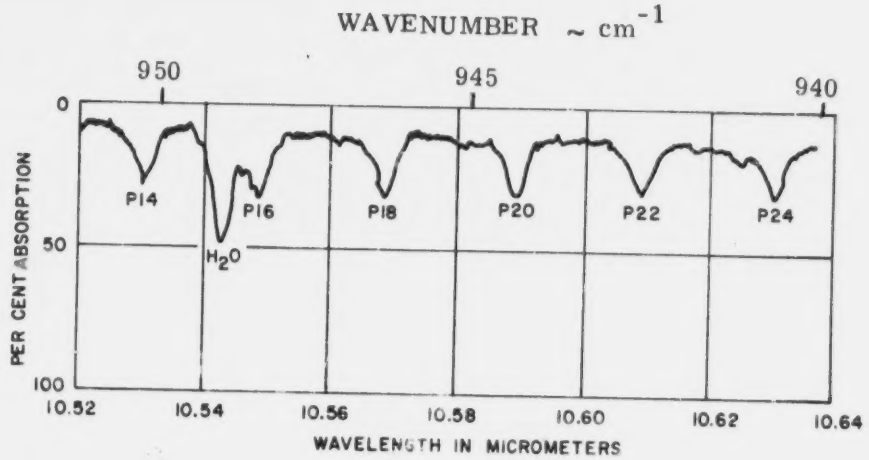

Figure 11. Carbon Dioxide Absorption and Water Vapor Absorption in Solar Spectra (4)

At long range and under conditions of high absolute humidity, there is an absorption due to the wings of the water vapor lines on either side of the 9 to 11 micron atmospheric window. The absorption coefficients for water vapor and carbon dioxide have been measured by McCoy et al (5) at the 10.59 micron and 9.51 micron lines of the CO_2 laser. Their data for the 10.59 micron line are presented in Table V and Figure 12. Because of the extremely strong self pressure broadening effect, the transmission of water vapor in air does not vary exponentially with the precipitable centimeters of water in the path, as Beers law would predict. However, this effect does not introduce nonlinearity in the system response. The measured absorption coefficients for the expected range of partial pressures at 9.55 microns are 80% as large as those at 10.59 microns. That is, $\alpha_{9.55}/\alpha_{10.59} = 0.80$. This ratio remains constant as a function of partial pressure, as can be seen from Figure 13. In other words, the absorption pattern in the form of the natural log of the transmission at each wavelength does not change with large concentrations.

In the selection of a group of four laser lines, then, the only spectral interferents that were considered were ozone and water vapor. Of course, ammonia must be considered as a spectral interferent for the detection of ethylene and, similarly, ethylene is an interferent for ammonia.

Before the beginning of the contract effort, a two-wavelength selection computer run was made to choose the best wavelength pair for ethylene detection from 70 CO_2 laser lines, assuming 14 spectrally interfering absorbers. They include the absorbers listed in Table VI, plus two absorbers (carbon monoxide and nitric oxide) that do not absorb in the 9-to-11.5μ region and can be ignored. The two wavelengths chosen were 10.532μ and 10.675μ. The (λ vacuum) values in Table VI indicate the relative system response to equal quantities (CL) of absorbers. The most significant interference is propylene, whose response is approximately 1/40 that of ethylene. This rejection is not sufficient for operation in an environment where propylene might occur in concentrations equal to or greater than that of ethylene. For example, 10 ppm of propylene would give approximately a 25% error in

TABLE V

10.59μ WATER VAPOR AND CO_2 EXTINCTION COEFFICIENTS AND LOSS PER KILOMETER AT 25°C (77°F)

RELATIVE HUMIDITY (%)	k (km^{-1})	k (ft^{-1})	loss ($dB\ km^{-1}$)
10	0.0125	3.81×10^{-6}	0.054
20	0.0338	1.0×10^{-5}	0.15
30	0.0653	1.99×10^{-5}	0.28
40	0.107	3.26×10^{-5}	0.46
50	0.157	4.78×10^{-5}	0.68
60	0.215	6.56×10^{-5}	0.93
70	0.284	8.65×10^{-5}	1.2
80	0.363	1.11×10^{-4}	1.6
CO_2 at 330 ppm:	0.0811	2.48×10^{-5}	0.35

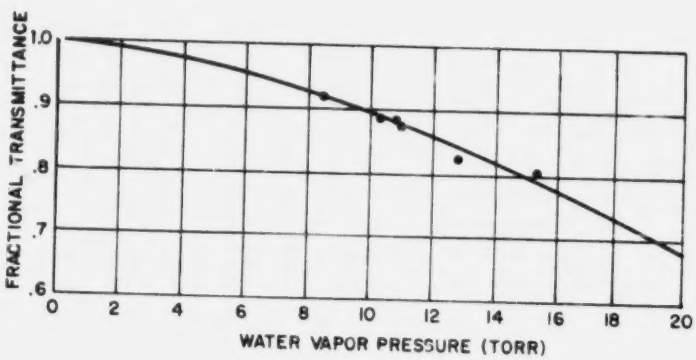

Figure 12. Measured 10.59μ Transmittance of Water Vapor in Air at 23°C vs. the Partial Pressure of Water Vapor for a 980-m Path. Total pressure = 700 Torr

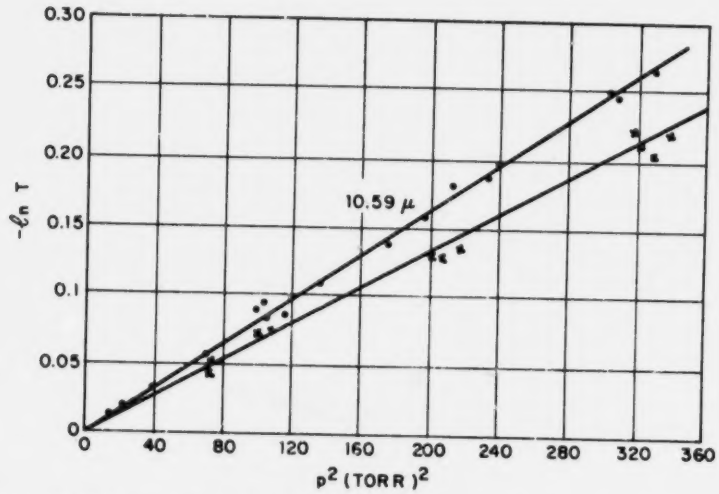

Figure 13. The Logarithms of the 9.55μ and 10.59μ Transmittance of Water Vapor at 25°C vs. Pressure for a 980-m Path

TABLE VI

RELATIVE SYSTEM RESPONSE ASSUMING TWO WAVELENGTHS

POLLUTANT	Detect Ethylene With 10.675μ And 10.532μ RESPONSE
Ethylene	36.703
Ozone	0.000
Ammonia	-0.103
Benzene	0.000
Butane	0.627
Ethane	0.003
Nitrogen Pentoxide	0.068
Propane	-0.325
Propylene	-0.884
Sulphur Dioxide	0.000
Sulphur Trioxide	0.006
Toluene	-0.565
Water Vapor	0.003

estimating 1 ppm of ethylene. If 10 ppm of propane and toluene were also present, the error would be approximately 50%. Increasing the number of wavelengths increases the rejection of interferences, but adequate rejection depends on the accuracy and range of estimation and the number of interferences.

Another two wavelength selection computer run was made to choose the best wavelength pair for ammonia detection assuming the same 14 spectral absorbers. Several pairs of wavelengths chosen were almost equally good. One of those pairs were 10.719μ and 10.675μ. It was decided at that point to choose these two wavelengths plus 10.532μ for the detection of ethylene and ammonia and rejection of water vapor and ozone. There were several reasons for this decision:

1) At these three wavelengths, neither water vapor nor ozone produce spectral interference

2) To the extent that the gases listed in Table VI are representative, the rejection of pollutant gases having any spectral absorption in the 9 to 11 micron wavelength region is high

3) Direct measurements with the laser and a gas cell indicate that the P-14 line at 10.532μ and the P-32 line at 10.719μ give the maximum absorption coefficients for ethylene and ammonia, respectively, of any of the spectral lines available from this laser. This is in spite of the fact that the measured absorption spectra of Figure 7 seem to show that the P-34 line at 10.742μ coincides better with an ammonia absorption peak

4) Both ammonia and ethylene absorbed on only one of the three lines and showed extremely small absorption on the other two lines.

5) The fact that these lines are close together should provide better rejection of spectral interferences such as particulate matter that do not exhibit fine structure but change their transmittance rather slowly with wavelength.

Because the three wavelengths chosen appeared to be able to handle the problem as modelled very adequately, the decision as to the fourth wavelength was arbitrary. Nothing could be gained in terms of sensitivity and selectivity in the detection of ethylene and ammonia by judicious selection of the fourth wavelength. The choice of 9.505 microns (10.532 cm^{-1}) was made for two reasons:

1) We wished to observe the response of the system to scintillation for wavelengths that were more widely separated

2) 9.505 microns could be used for the detection of ozone or water vapor if we so desired.

Table VII summarizes the measured absorption coefficient data on the four wavelengths. The coefficients for ethylene and ammonia were measured directly with the laser and a gas cell here at the Electronics Laboratory. The data on ozone were taken from the spectra measured by Hanst [1]. The absorption coefficients for water vapor were taken from McCoy [5].

TABLE VII

MEASURED ABSORPTION COEFFICIENTS

Wavelength ~ microns	9.505	10.532	10.675	10.719
Wavenumber ~ cm^{-1}	1052.1	949.5	936.8	932.9
α (ethylene) ~ $(atm\text{-}cm)^{-1}$	1.1	48	2.0	2.4
α (ammonia) ~ $(atm\text{-}cm)^{-1}$	0.9	2.0	1.1	27
α (ozone) ~ $(atm\text{-}cm)^{-1}$	25	0	0	0
α (water vapor) ~ $(atm\text{-}cm)^{-1}$*	2.6×10^{-6}	3.2×10^{-6}	3.2×10^{-6}	3.2×10^{-6}

* The absorption coefficients for water vapor are a function of partial pressure, as explained previously. The above data were for a partial pressure of 17.5 torr, which is equivalent to 100% RH at 68°F, 74% RH at 77°F or 5.7 precipitable centimeters over a 1 Km. path.

F. SELECTION OF LINEAR WEIGHTS

We have used two techniques that maximize the signal-to-noise ratio for the detection of a single pollutant in the presence of some complex environment. The first technique finds a vector normal to the "plane" of spectral interferences that maximizes the response to the gas. The second technique maximizes the signal (for the detection of the pollutant) divided by the standard deviation of the effective noise distribution of the environment. The effective noise distribution of the environment represents variations due to a superposition of some combination of detector noise, known spectral interferences, unknown spectral interferences, and optical (e.g., scintillation) noise.

The covariance matrix can be used to represent the effective "noise" distribution of the environment. A four-by-four matrix is used to represent the variances and covariances of the noise at the wavelengths. Once the specific laser wavelengths have been chosen, the optimum linear weight can be found rapidly on the GE 635 computer.

Several sets of weights were calculated for a variety of assumed conditions. Typical results are presented in Table VIII. Spectrally neutral attenuation is always considered one of the spectral interferences. In spite of the fact that, by definition, its transmission does not vary spectrally, it must be discriminated against. A one-wavelength system, for example, could not distinguish between neutral attenuation and the gas that absorbs specifically at that wavelength. Neutral attenuation is produced by particulates in the air, angular misalignment of the optics, any obscuration in the path, dirt on the optics, change in responsivity of the bolometer, or change in the gain of the preamplifier. From the absorption coefficients, it is seen that, using these four wavelengths, ozone is the inverse of a combination of water vapor and neutral attenuation. For this reason we can detect ethylene, for example, uniquely in the presence of four spectral interferences (i.e., ammonia, ozone, water vapor and neutral attenuation) with just four wavelengths. Table VIII gives some calculated weights for the detection of ethylene, ammonia and also ozone. This table is the result of just one of several computer runs to determine the optimum linear weight for different models of the spectral environment. The results were dependent upon the relative magnitude of the random spectral interferent assumed, the model for the spectral distribution of the interferent, and the magnitude of the other interferents. The calculated sets of optimum linear weights, for the case where the random spectral interferents had approximately equal magnitude to that of ethylene, ammonia and ozone, were for all practical purposes identical to those listed in the first part of Table VIII. In other words, only 10.53 and 10.67 microns are used in detecting ethylene, and 10.719 and 10.67 microns are used for detecting ammonia. These results are what one would expect intuitively. The wavelength corresponding to the absorption peak and the nearest available other wavelength are optimum. Our experience with optimizing the detection of chemical warfare agents indicates that things usually do not work out so simply.

TABLE VIII. SETS OF OPTIMUM LINEAR WEIGHTS

Wavelength	9.505	10.532	10.675	10.719
Wavenumber	1052.1	959.5	936.8	932.9
Independent Detection of Ethylene, Ammonia and Ozone with no random spectral interferences				
Ethylene	$+2.27 \times 10^{-11}$	+0.682	-0.658	-0.024
Ammonia	$+1.3 \times 10^{-10}$	-0.012	-1.39	+1.40
Ozone	+0.437	+0.0082	-0.448	+0.0025
Detection of ethylene and ammonia assuming only a large random spectral interference				
Ethylene	-0.225	+1	-1.59	+0.821
Ammonia	-0.057	+0.139	-1.08	+1

V. TEST PLAN

A. OBJECTIVE

The purpose of this plan was to define the equipment and procedures to be used in calibration of the laser system, measurements of the atmosphere and analysis and reporting of data.

B. EQUIPMENT

Measurements were obtained at two locations; at the General Electric Cazenovia Test Site for calibration and baseline measurements in a pollutant free environment, and at an urban site at Syracuse, New York, for measurement in the presence of pollutants of interest and ambient interferences.

1. Cazenovia Test Site

   a. General Electric "V" laser system including laser, retrotelescope and signal processor.

   b. Six-inch-diameter, twenty-seven-foot-long gas cell.

   c. Recorders:

      1) Two dual-channel Mark II Brush Recorders.

      2) One dual-channel Sanborn model 320 hot-pen recorder

      3) One eight-channel Sanborn hot-pen recorder

   d. Tektronix 541 Oscilloscope with Type CA Dual Trace Amplifier

   e. Ammonia and ethylene test gas samples and Hamilton sample handling syringes

   f. Meteorological instruments

      1) Thermometer,

      2) Hygrometer, Serdex model 201

      3) Anemometer, Lafayette and Taylor

   g. Varian Aerograph Gas Chromatograph, model 1520-1B with flame ionization detector

   h. Hamilton air sample syringes.

2. Urban Site

The same equipment as at the Cazenovia Test Site except as listed below.

a. Recorder - A Sanborn 8-channel recorder will replace the three test site recorders

b. The twenty-seven-foot gas cell will not be installed at the urban site

c. A six-inch-long gas cell will be used instead

C. MEASUREMENT PROCEDURES

1. Cazenovia

a. Laser Calibration

Calibration against specific gases was accomplished by injecting a measured sample of the specified target gas into the test cell and recording system response. The sample was allowed to diffuse through the cell for ten or fifteen minutes to observe: 1) the effects (if any) of dilution of gas within the cell upon system response, and 2) change in the system noise and system drift (if any) that occurs when an absorption signal is present.

The gas cell is a twenty-seven-foot section of six-inch-ID circular copper waveguide. The cell windows are 0.6 mil (0.0006 inch) polyethylene (handy-wrap or baggies). The reflection losses from these windows are somewhat spectral due to the interference between the front and back surface reflections. This spectral interference varies across the surface of the polyethylene because of non-uniformity in thickness. The spectral unbalance due to these windows was balanced out when the cell was set up and does not affect the system sensitivity or signal-to-noise except for a slight loss in total power received. An exhaust blower is mounted on the outside of the test cell at one end and an exhaust port at the other. The exhaust fan drives ambient air into the cell and out the exhaust port. When not exhausting, the blower was turned off and covered with a polyethylene bag and the three-inch-diameter port was sealed with a rubber septum.

To inject the test sample of gas, a sample cell with a silicone rubber septum was mounted onto the lecture bottle containing the pure test gas, i.e., ethylene or ammonia under pressure, and filled with the pure gas. The gas was extracted from the cell with a ten-milliliter hypodermic syringe through the septum and a measured amount injected

through the rubber partition on the exhaust port. When calibrating for ammonia it was found necessary to saturate the test cell walls with ammonia in advance of the calibration test to prevent rapid adsorption of the test gas sample onto the cell walls. This step was not necessary with ethylene.

After fifteen minutes of data recording, the exhaust blower and exhaust port were uncovered and the system flushed with outside air. This exhaust system removes more than ninety percent of the gas in the cell in ten seconds.

After flushing for two minutes, the blower was shut off, the ports closed and the zero condition of the system recorded.

b. Laser Baseline Measurements

Field data was recorded by strip chart recorders which continuously monitor the signal outputs from the absorption meters and the synchronous detector outputs during each test run. In addition, the average peak-to-peak signal return from the retroreflector was recorded on some tests. All meteorological data as indicated on the data format was recorded by hand.

Following calibration, the procedure was to first record any change in balance since the previous test, turn on the chart recorders and then record the meteorological data. The frequency with which weather information was recorded depended on how rapidly conditions were changing.

The laser was then peaked up by adjusting the vernier aiming mechanism (which directs the angle of the transmitted beam in azimuth and elevation) to determine if the unbalance was in any way related to an optical misalignment. Any change in balance caused by peaking was then recorded. The balance control dial settings were recorded, the system was balanced by resetting the dials and the new settings were recorded. These balance dials compensate for any spectral absorption signal due to fixed elements in the optical path such as lenses, coated mirrors and polyethylene windows. After balance, the four synchronous detector output meters read zero. The system was then left on with the recorders running for a minimum of two hours. During this time, surveillance was maintained and any changes in operating conditions that might affect the system were noted on the chart paper along with the time. The chart speed is one millimeter per second on the narrow chart paper and 1/4 mm/sec on the wide paper unless otherwise noted on the chart paper. At the end of the run, the recorder sensitivity

setting (volts/centimeter), the time and the data were recorded. Weather conditions were recorded again only if conditions had changed during the run.

In addition to the meteorological data already described, an attempt was made to measure the temperature gradient in the air near the optical test cell for the laser transceiver. Six thermometers were placed every two feet on a vertical ten-foot pole and shielded from heat radiation from the ground, sky and sun. The thermometers were read during conditions of both high and low optical noise (scintillation). Less than $1/2^{\circ}$ F was observed.

c. Supplementary Measurements

Independent measurements of ethylene concentration were made on ambient air samples taken at the two ends of the two-mile test path. Meteorological conditions were also measured at each end of the path including temperature, wind speed and direction, cloud cover, humidity, subjective measures of atmospheric scintillation and solar conditions; and time was recorded for all tests. (See IV - Data Recording.)

Independent measurement of ethylene concentration was made as follows:

1) Air samples were taken with a one-liter Hamilton syringe and pumped into a Saran sample bag. Sample size was about five (5) liters. Anspec Company 12-liter bags were used.

2) Filled sample bags were returned to the Technical Services Laboratory. Sample bags were kneaded briefly to insure mixing of the sample constituents and a 1 to 10 milliliter sample extracted with a 10-ml Hamilton syringe. Sample extraction was at room ambient temperature.

3) The extracted sample was injected into the gas chromatograph. The peak height of the ethylene peak on the GC output recorder was used to indicate the concentration of ethylene in the sample.

4) The GC was calibrated before and after sample measurements using a standard gas mixture purchased from Matheson Company. The standard gas contains 5 (five) parts per million by volume of ethylene gas in dry nitrogen gas. This standard gas is diluted with dry nitrogen gas to obtain standard concentrations of ethylene in concentration ranges of interest, i.e., comparable to the samples being measured.

No satisfactory independent test for ammonia concentration at the levels of interest was found.

2. Urban Site

a. Laser Measurements

The urban measurements procedure was identical to the procedure used at the rural site except for two differences. The test cell was six inches long instead of twenty-seven feet and an absolute zero reference calibration was made to isolate any spectral effects other than those caused by absorbing materials in the air.

The six-inch test cell was calibrated against the twenty-seven-foot test cell at the rural site to insure that no unforeseen effects take place such as signal variations caused by changes in concentration for the same optical thickness of the gas. This six-inch-long cell also had polyethylene windows and a rubber partition for sample injection.

Absolute calibration of the system was established using a portable retrotelescope at approximately five hundred feet (a short path) and comparing the long-path and short-path signals. By making the short path optically similar to the long path, the only differences in the two conditions is the thickness of the air sample measured (see page 47). By extrapolating the two readings obtained to zero air thickness, a zero baseline is obtained. This calibration technique was tested at the rural site before moving into the urban area.

At the urban site, measurements were made of both ammonia and ethylene; however, only the latter was used for analysis and system performance evaluation. For ammonia we correlated readings with known test cell concentrations.

b. Supplementary Measurements

Once the baseline was established, calibration and measurements proceeded exactly as at the rural test site. The supplementary measurements were taken at the end points of the test path and at several points along the path.

D. DATA RECORDING

1. Data Format

A standard data sheet for recording measurement is shown in Table IX. In addition to the data sheet, an 8-channel strip chart recording was made of the variables vs. time listed on the page following Table IX.

TABLE IX. STANDARD DATA RECORDING SHEET

LASER AIR CONTAMINANT MONITOR

Test Number _____

Date _____

Location _____

- General Weather Conditions

  Precipitation

  Visibility

  % Cloud Cover

- Local Weather Conditions

	Transmitter	Retroreflector
Time		
GC Ethylene Measurements		
Wind Speed/Direction		
Temperature		
Humidity		

- Calibration and Measurement

  Cubic Centimeters of Gaseous Ethylene Injected _____ cm^3

  Cubic Centimeters of Gaseous Ammonia Injected _____ cm^3

Synchronous Detector	Relative Transmission Before Peaking	Relative Transmission After Peaking
9.505μ		
10.532μ		
10.675μ		
10.719μ		
Absorption Meter		
Ethylene		
Ammonia		

Comments

Synchronous Detector Output Voltages:

a. 9.505μ wavelength

b. 10.532μ wavelength

c. 10.675μ wavelength

d. 10.719μ wavelength

Absorption Meter Voltages:

e. Ethylene

f. Ammonia

Reference Voltage:

g. Average received laser power

h. Spare channel (seldom used)

2. Ambient Conditions

Consistent with available weather conditions during the test periods, data runs were made during daytime, dusk and nighttime for as wide a variety of ambient weather conditions as possible. It was not possible to obtain data for all the combinations of weather conditions.

At least 2 hours of continuous data were taken for each data run and a minimum of 24 hours total of data were taken. For each of the conditions listed below, data were taken at midday, dusk, and after dark.

a. Clear sky - less than 25% cloud cover. Wind zero to five mph

b. Heavy overcast but no observable precipitation. Wind zero to five mph

c. Clear sky - less than 25% cloud cover. Moderate to high winds - fifteen mph or greater

d. Heavy overcast with moderate to high winds

e. Precipitation - light snow flurries and high winds

f. Precipitation with low wind conditions

E. DATA ANALYSIS

The objective of the data analysis was to evaluate the performance of the laser air contamination monitor under a variety of environmental conditions and to determine which of those conditions influenced the behavior of the laser system. Two kinds of error were measured in this evaluation. One was short-term signal fluctuation or noise such as is produced by system noise and atmospheric scintillation. The other was long-term drift or apparent absorption signal which is undistinguishable from absorption signal. These two noise phenomena are different only in the length of time involved, but the distinction is convenient. The data is presented in graphical form, and also tabular form, to show the correlation between the following parameters:

Signal-to-noise vs. atmospheric scintillation

Signal-to-noise vs. signal level returned (atmospheric transmission)

Signal-to-noise vs. each of an assortment of weather conditions

Long-term drift or signal unbalance vs. weather conditions

Long-term drift or signal unbalance vs. scintillation

Long-term drift or signal unbalance vs. signal level

Noise and drift vs. time between measurements

VI. RURAL TEST SITE MEASUREMENTS PROGRAM

A. SUMMARY OF RURAL TEST RESULTS

At Cazenovia, New York, the laser site and the retroreflector site were each located on top of a ridge 9, 800 feet apart and separated by a valley approximately 500 feet deep. Data were taken from November 1970 through April 1971 under the full range of weather conditions available during this time.

Over the five-month period, more than sixty hours were spent recording or attempting to record data. These data were taken under both clear sky and overcast sky, with and without precipitation. Atmospheric scintillation was measured by fluctuations in the return signal level, both on the oscilloscope that monitors the return signal directly, and also on the signal level indicator that is recorded on one strip chart. The signal level indicator recorded variations in the average signal level with a ten-second time constant. Scintillation was highest during the conditions of clear sky, at mid-day and, on two occasions, around midnight; while at dusk, the scintillation was minimum. The correlation between the scintillation magnitude and errors or pseudo-absorption signals on the signal processor output was high.

During conditions of maximum scintillation, we detected five parts per million of ethylene and seven parts per million ammonia in the twenty-seven-foot test cell. The measured absorption signals for these concentrations were ten times the RMS error occurring during times of maximum scintillation and atmospheric turbulence. To produce the same absorption signal, the average concentration over the entire ten-thousand-foot range over which we were operating would require only fourteen parts per billion of ethylene and nineteen parts per billion of ammonia.

The data taken at the rural site clearly indicate the following about the limit of the detectability of the system:

1) The accuracy with which we could reliably measure the average concentration of ethylene and ammonia over the path was determined by the optical noise and scintillation produced by atmospheric turbulence and temperature gradients in the path.

2) All the recorded data taken with both test cells confirmed the fact that the calibration of the system never varied. The inside diameters of both test cells, the 6-inch cell and the 27-foot cell, were 6 inches. One milliliter of gas, either

ethylene or ammonia, injected at atmospheric pressure, produced an optical thickness (concentration times path length) of 0.0055 atmosphere-cm. Each milliliter of ethylene always yielded α CL = 0.25 and each milliliter of ammonia always yielded α CL = 0.15. Temperature effects due to change in density with temperature and doppler broadening were too small to measure.

3) The signal level returned from the retroreflector two miles away was more than two-hundred times larger than that needed for good operation of the system. Attenuation of the signal by rain, haze or snow, up to two-hundred to one, had absolutely no effect on system performance.

4) When the attenuation was greater than 500:1, or rather when the signal level at the output of the preamplifier dropped to less than 100 millivolts, the system became inoperable because of internal system (detector) noise.

B. RURAL TEST SITE

The rural test site is located at General Electric's Antenna Test Facility on U.S. Route 20, about 15 miles southeast of Syracuse, New York, near the town of Cazenovia. It consists of a transmit site and a retroreflector site, each located on top of a ridge, and separated by a valley approximately 500 feet deep. Figure 14 shows the profile of the terrain separating the two locations. The 9,800-foot separation between the transmit site and the receiver site is an excellent range for evaluating the ILAMS performance. The sparse rural population, remote from any major sources of air contamination, provides a relatively clean atmosphere in which to measure data independent of the interfering effects of pollutants. All the ethylene point measurements made at this Cazenovia test site registered zero ethylene. This indicates that the concentration was below 5 ppb. Since there were few roads and little traffic in the area, this result is not surprising. Figure 15 shows an aerial view across the valley as seen from above the ILAMS transceiver.

The ILAMS transceiver was located in a heated, insulated room in a pole barn with a concrete floor; see Figure 16. The beam was transmitted through a 0.0006" polyethylene window, and then through the twenty-seven-foot gas cell and across the valley to the retroreflector. The gas cell can be seen in Figure 17.

The retroreflector was mounted on the eastern side of the valley at the same altitude as the transceiver, in a small unheated building with an open window. A shield was placed over the window to keep snow from blowing into the retrotelescope.

C. RURAL TEST RESULTS

The goal of the rural test program was to evaluate the system performance in a clean-air environment. The objectives were to study and measure the behavior of the ILAMS while it was isolated from the effects of airborne contaminants and particulates, and thereby provide a baseline from which to judge the data taken in the urban environment. There are two major differences between the rural and urban environments that would influence the system performance.

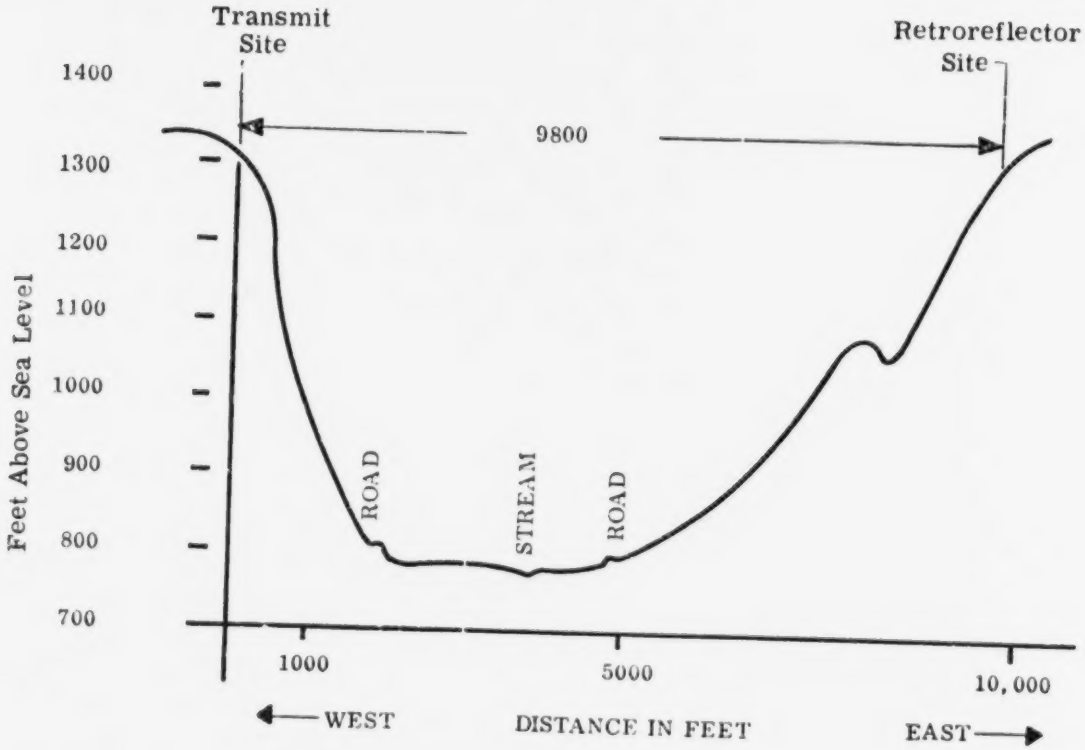

Figure 14. Rural Test Facility Profile

Figure 15. Photo of Cazenovia Valley

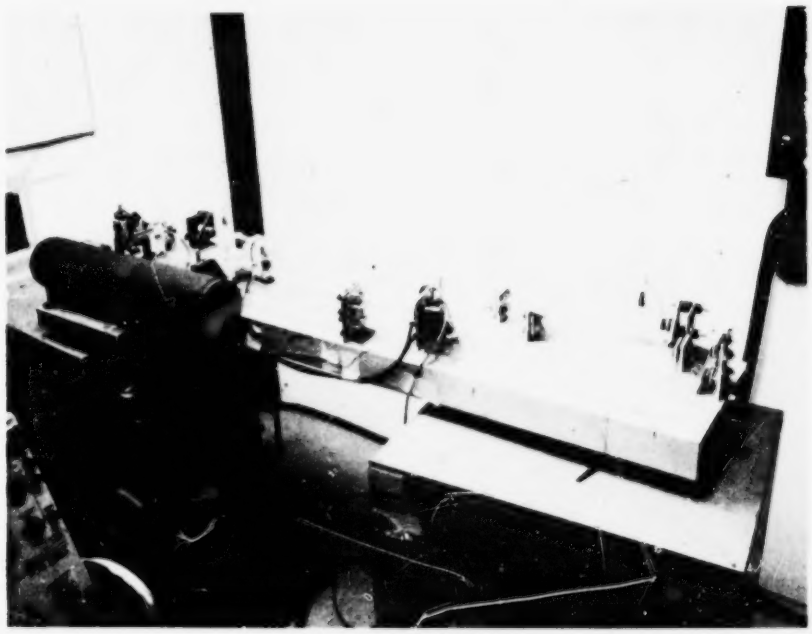

Figure 16. ILAMS Transceiver and Recording Equipment at Rural Test Site

Figure 17. 27-foot Gas Cell at Rural Test Site

First, the urban airborne contaminants might have unknown spectral absorption patterns that would produce false signals. Secondly, the atmospheric turbulence that produces scintillation of the return signal is more severe in the urban environment, particularly when the path of the monitoring beam passes over large buildings and industrial sites.

The emphasis in the rural measurements program was to measure the noise and drift in the system output. Noise and drift represent the measurement error and establish the detectivity or minimum detectible signals that can be used reliably as an indication of average pollutant concentration along the monitored path. These errors were measured and correlated, where possible, to the environmental effects that produced them. In some cases, the mechanism by which such noise and drift were produced was studied so as to (1) improve our confidence in the validity of the results and (2) project improvements in the system and estimate the potential detectivity of the post-breadboard system.

The limit of the detectability of the system, that is, the accuracy with which we could reliably measure the average concentration of ethylene and ammonia over the path, was determined by the optical noise and scintillation produced by atmospheric turbulence and temperature gradients in the path. Spectral attenuation -- attenutation at some wavelengths more than others -- is the information used by the ILAMS to measure the amounts of particular gasses in the air. Attenuation due to absorption by a known gas occurs in predictable spectral patterns and is used to identify or discriminate against the gas. Random attenuation, such as that caused by atmospheric scintillation or by internal system noise, represents an error and limits the sensitivity of the system.

The spectral attenuation can be produced by the atmosphere in several ways. The measured intensity distribution of a cross-section of the laser beam at the output of the beam expander shows that the pattern is not as symmetrical as one would expect for a TEM_{00} mode. Contours drawn through areas of constant power density, in Figure 18, show differences in the beam patterns in the near field for each of the four wavelengths; consequently, the far-field patterns would also exhibit differences. Therefore, amplitude modulation of the signal is produced by translation or distortion of the beam pattern at the retroreflector, as might be caused by atmospheric effects. If the patterns are different for the different wavelengths as is indicated by the measured difference at the beam expander -- then the modulation at each wavelength is different and such modulation is an error -- that is, it cannot be distinguished from an absorption pattern. Atmospheric scintillation due to air in the immediate vicinity of the retroreflector can have similar adverse results on the illumination of the receiver. The data that have been accumulated indicate that it is these atmospheric effects, particularly those near the beam expander and near the retroreflector, that are the dominant effects responsible for the noise and drift recorded on our data.

In order to reduce the scintillation to reasonable levels, it was necessary to isolate the test cell from sunlight and reflected sunlight and locate the cell away from the building so that the cell window did not come into contact with room air at a temperature different from that of the air inside the cell. A separate polyethylene window was installed across the window of the room

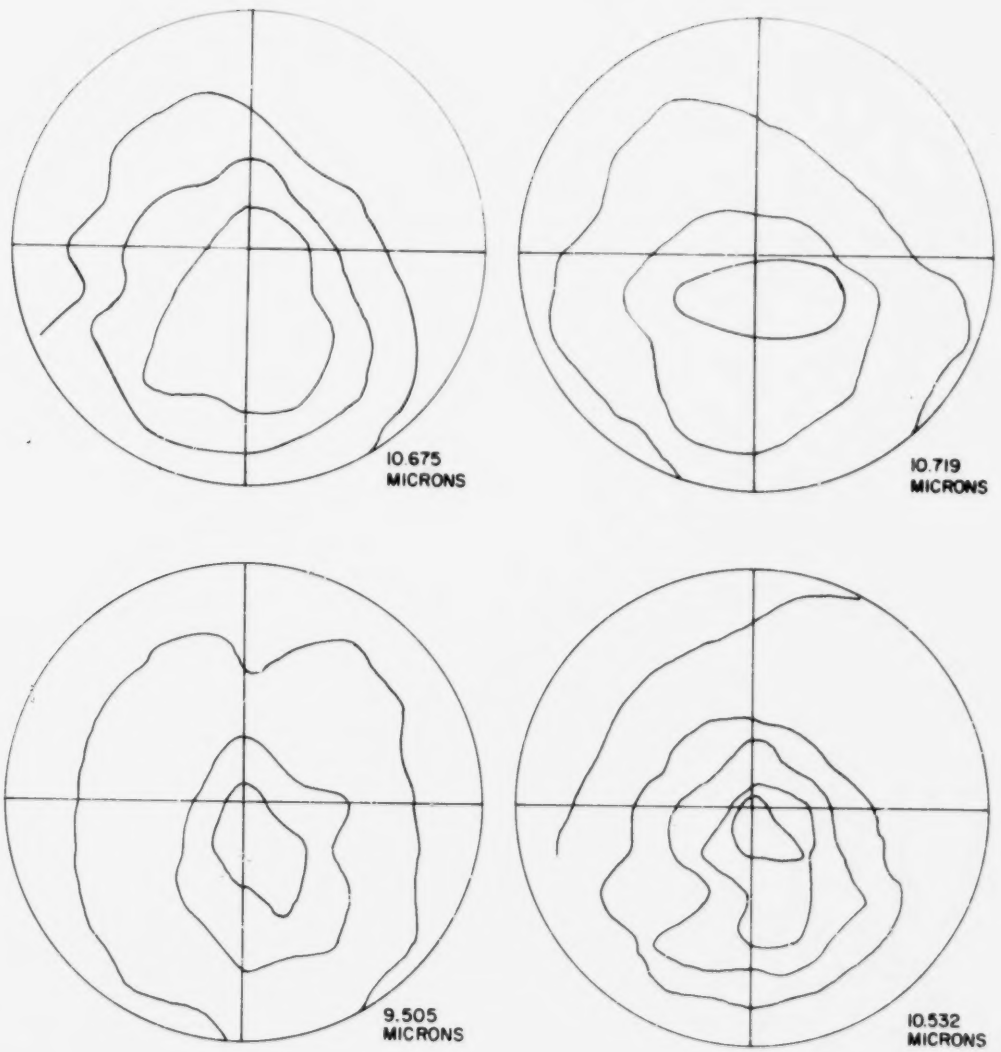

Figure 18. Contours of Equal Power Density at the Beam Expander Output

through which we transmitted and received, to prevent mixing of room air and outside air in the path of the laser.

Two types of retroreflectors were used with grossly different results. A mosaic of thirty small cube corners with a total capture area of one square foot was used initially. This reflector resulted in one-hundred-percent modulation of the energy returned to the system at each wavelength on a clear but windy day, and the modulation (or scintillation) at each wavelength was apparently independent, producing large errors. In other words, the scintillation was highly spectral. The term "scintillation" as used here refers only to fluctuations in the peak amplitude of the signal at the output of the pre-amplifier as observed on an oscilloscope. The dual-beam oscilloscope is synchronized to the chopper wheel so that one sweep is produced for each rotation of the chopper. The reference (transmitted) energy and the return signal were presented together on the separate traces, so that the two signals could be compared rapidly on a wavelength-to-wavelength basis. The output of the reference detector (as seen at the output of preamplifier B) remained constant, while the signal return fluctuated in amplitude. When a nearby retroreflector, mounted fifty feet from the transceiver, was used, no amplitude fluctuation occurred. The retrotelescope across the valley was mounted on a concrete pedestal in the ground. Therefore, the amplitude fluctuations were attributed to atmospheric turbulence and are called (for convenience) scintillation. Two types of scintillation effects, spectral and non-spectral, were noted. Non-spectral amplitude fluctuations affected all wavelengths together, like a rapidly changing neutral attenuation. This type of scintillation is not recorded by the system because of the action of the AGC and also because the weights are chosen to discriminate against neutral attenuation. Therefore, the non-spectral scintillation produced no error*. The spectral type of scintillation did produce system error. The short-term spectral fluctuations were averaged out by the three-second integration time of the instrument, while the longer-term fluctuations appeared as false absorptions. When both kinds of scintillation occurred together, as they usually did, a rough estimate could be made as to their relative magnitudes, by observing the oscilloscope.

It was found that, by shaking the cube-corner mosaic back and forth either vertically or horizontally across the beam, the scintillation magnitude could be reduced by a factor of three to one, and the spectral component only accounted for about fifty percent of that modulation. In other words, while shaking the cube corners, the modulation of the signal due to scintillation was about 35% rather than 100% and only partly spectral. Moving the cube-corner mosaic towards and away from the transceiver at the same rate yielded no improvement over holding it still. The improvement is attributed to time averaging of the interference fringes as they change rapidly with cube-corner motion.

A substantial improvement (20% modulation under the same weather conditions) in the magnitude of the scintillation noise was achieved by using a 12" aperture telescope with a mirror at the image of the laser transmitter as a retroreflector. One such retroreflector was described, in Section III, as a "cat's eye" retroreflector. Two other telescopes have been used as retro-reflectors in the course of these experiments. A 12"-aperture Dall-Kirkham

* This statement is not precisely true. If some of the scintillation noise occurs at the chopping frequency, 75 Hz ± 0.2 Hz, it will produce an error. This effect is relatively small.

with a three-inch-diameter secondary and an effective focal length of 16 feet was used with a plane mirror at the image point. A 12" aperture parabola with a six-foot focal length and a two-inch-diameter "45°" mirror five feet from the parabola was also used, with a plane mirror at the image plane. All three of these retrotelescopes appeared to work equally well and all were easy to align and aim. It was found to be very important, however, that the mirror be located at the image point of the transceiver, and not at the focal point of the telescope or at any other point. One reason for this is that the best focussing of the return energy occurs at this alignment; so, for long-range work, the maximum energy is returned to the receiver. A more important reason turned out to be that, for locations of the mirror other than at the transceiver image plane, the obscuring shadow of the secondary mirror in front of the aperture of the telescope is "imaged" back on the transceiver aperture. For this case, no signal, or only a reduced signal, would be returned to the ILAMS transceiver unless scintillation was present. Such a design maximizes the scintillation noise. The retrotelescopes were aligned by adjusting them for maximum signal return to the transceiver. It was observed that this peak also corresponded to minimum scintillation noise on the oscilloscope.

The major difference in the performance of the two types of retroreflectors was not in the percent modulation of the return signal, but in the spectral content of such modulation. Using the retrotelescope, the correlation between the optical noise at the four wavelengths was high. That is, the modulation appeared to be very neutral spectrally. The correlation coefficient between the noise at any two of the wavelengths used was approximately 90%, whereas the noise at each wavelength, using the mosaic of cube-corner reflectors, appeared to be statistically independent. This difference is, of course, crucial to the system operation. The correlated (wavelength-to-wavelength) component of the noise, whether it be at high frequencies or low enough to represent drift, does not produce a system error, except when the frequency of the scintillation falls within the narrow pass-band of the system (0.2 Hz) centered at the chopping frequency (75 Hz).

The available signal, when operating over the two-mile range at Cazenovia, N.Y., was several hundred times the minimum usable signal. That is, the system always operates with no decrease in detectivity under conditions of up to five hundred to one reduction in the amplitude of the signal return. As long as the signal return is sufficient to produce a 0.1 volt signal at the preamplifier output for every pulse, the system noise has no measurable effect on performance. However, for weaker signals than this, the system error increases greatly due to internal system noise, and the ILAMS is no longer operable. No useful data were recorded for signals weaker than 0.1 volts (measured at the preamp output). The reason for this abrupt low-signal threshold is that the log amplifier goes into saturation when faced with a zero or negative voltage input. When the sum of the signal plus the zero-mean system noise goes below zero, the log amplifier saturates and produces a large error because of its slow recovery. Since the peak-to-peak system noise measured at the preamplifier output is 0.16 volts (160 millivolts) with these detectors, the log amplifier frequently goes into saturation when the signal level drops to near that value. The detector noise is two orders of magnitude larger than any of the other sources of internal noise, so that an improvement in NEP of the detectors by 100:1 would improve the low-level signal threshold accordingly.

Such detectors are available in thermistor bolometers as well in cooled photoconductors. Reduction in signal was often caused by rain, fog, or snow. The retroreflector was mounted in a small white building across the valley. We found that, in rain or snow, the system would operate at optimum detectivity until the building was no longer visible with the naked eye. If we could not see the two miles across the valley, the return signal from the retroreflector was usually too weak for reliable operation of the system. Under conditions of fog, however, the infrared transmission held up until the visibility was less than one mile, indicating that a large percentage of the fog particles were small enough (below ten micrometers diameter) to produce less scattering at ten microns than raindrops or snowflakes.

The dynamic range of this system can be expressed in terms of the response to concentrations of the target gases in the test cell. The system responds linearly to ethylene gas from a minimum detectable concentration of one part per million in the twenty-seven-foot test cell (2.7 ppb over the two mile range) to 53 parts per million in the test cell (144 ppb over the two mile range). The corresponding concentration range for linear detection for ammonia is 1.5 ppm to 80 ppm in the test cell, or 4 ppb to 216 ppb over a two-mile range. The linear range is limited by the electronics and not by saturation of the absorbing medium. The maximum signal that the electronics can tolerate for linear operation is 12 volts.

It is significant that, except for loss of signal because of weather conditions heavy enough to obscure good "seeing" of the retroreflector site, scintillation, and those atmospheric conditions known to contribute to scintillation, were the only factors that correlated with the signal-to-noise of the system. The data recorded indicates that the signal-to-noise was aggravated by sun loading of anything along the active path between the laser system and the retroreflector. Windows, building walls and the test cell were particularly susceptible. During periods of high wind, overcast sky or dusk, the scintillation magnitude was low. The improvement in system signal-to-noise, from times of high scintillation to times of low scintillation, was approximately five to one. At one point, we attempted to stop occasional water condensation on the retrotelescope by wrapping heating tape around the primary mirror. This had disastrous results on the magnitude of the scintillation noise and had to be discontinued. Temperature and humidity appeared to have no effect on signal-to-noise, and wind velocity had only a small effect (that of reducing the scintillation) under clear weather conditions during the day or late at night.

To present a clearer understanding of exactly what data were recorded and how, a reproduction copy of one of the chart recordings is included as Figure 19. This recording was made in April, during conditions of poor visibility. A light drizzling rain was falling, and the valley was sufficiently foggy for visibility to be a maximum of one mile and sometimes only one-half mile. The eight lines each represent a separate recording channel, as follows:

1. Average signal level returned from the retroreflector. The left-hand edge represents zero signal.
2. The log of the transmission of the path at 10.532 μm.

3. The log of the transmission of the path at 10.719 μm.

4. The log of the transmission of the path at 10.675 μm.

5. A weighted sum of the outputs of the four wavelength channels, designed to respond to ethylene and discriminate against ammonia, water vapor, and ozone.

6. A weighted sum of the outputs of the four wavelength channels, designed to respond to ammonia and discriminate against ethylene, water vapor, and ozone.

7. A weighted sum of the outputs of the four wavelength channels, designed to respond to ethylene and discriminate against ammonia and the small measured spectral unbalance associated with changes in the fog density across the valley.

8. The log of the transmission of the path at 9.505 μm.

Time proceeds from the bottom of the chart to the top. The horizontal grid lines each represent twenty seconds. The elapsed time of this chart recording is fifty-five minutes. At somewhat irregular intervals of approximately three minutes, we iniected one-half of a milliliter of ethylene gas at atmospheric pressure into the test cell up to a maximum of eight milliliters. Each one-half of a milliliter represents a concentration of 3.33 ppm in the 27-foot test cell, or 9 ppb over the two-mile range. Alternately, we injected one milliliter of ammonia gas at a time, also at atmospheric pressure, into the cell. Each cubic centimeter of ammonia represents 6.67 ppm in the 27-foot test cell, or 18 ppb over the two-mile range.

This chart record shows several things. The system gives a linear response over large ranges in concentrations. The noise and drift in the signal output are small compared with the injected gas concentrations, and the responses of the weighted output signals to ammonia and ethylene are independent, illustrating the ability of the linear weighting in the signal processor to discriminate between pollutant and potential interferences. Note the tendency of the ammonia to decrease due to absorption by the walls of the test cell. This occurs in spite of our preconditioning of the cell to ammonia gas. We have found that the cell walls come to equillibrium with the gas in the cell and therefore contribute to the gas in the cell if the vapor pressure of the absorbed ammonia is greater than the partial pressure of the ammonia gas in the cell. Because of this, we allowed the walls to absorb ammonia up to a maximum vapor pressure of one ppm. In the experiment recorded on this chart, the measured signal in the ammonia channel would have been approximately fifty percent larger than what is shown on the chart recording. Atmospheric scintillation was measured by fluctuations in the return signal level, both on the oscilloscope which monitors the return signal directly, and also on the signal level indicator that is recorded on the strip chart. The signal level indicator records variations in the average signal level with a ten-second time constant. (The other outputs are recorded with a three-second time constant.) Scintillation was highest during the conditions of clear sky, at midday. This was true on all our data runs. However, scintillation was sometimes found to be equally high at around

midnight under clear skies; while, at dusk, the scintillation was minimum both before and after dark. The correlation between the scintillation magnitude and error or pseudo-absorption signals on the recorded outputs from the signal processor output was high.

During conditions of maximum scintillation, we were consistently able to detect five parts per million of ethylene and seven parts per million of ammonia in the twenty-seven-foot test cell. The measured absorption signals for these concentrations were ten times the RMS error due to scintillation and atmospheric turbulence. To produce the same absorption signal, the average concentration over the entire ten-thousand-foot range over which we are operating would be fourteen parts per billion for ethylene and nineteen parts per billion of ammonia.

During the day- and night-time measurements, thermometers were set up along a support structure shielded from thermal radiation. The purpose of this experiment was to measure the vertical temperature gradient across the monitoring beam during conditions of both high and low scintillation. Four thermometers were located at one foot, four feet, seven feet and ten feet from the ground. The thermometers are bulb/capillary alcohol thermometers. Because relative temperature between thermometers is of primary interest, they were calibrated against each other, but not against an absolute standard. The data taken indicated less than one-half degree difference over the ten-foot path, which is low compared to temporal fluctuations in temperature over short periods of time. The experiment was discarded as fruitless.

Two types of portable retro-telescopes (a single cube corner and a small retro-telescope) were set up at approximately five-hundred feet from the transmitter, at the rural site, in order to test the absolute calibration technique. The cube-corner retroreflector was shown to have sufficiently good optical and diffraction properties for use at this close range. The interference phenomenon that we observed with a cube-corner mosaic at long range was not present to a measurable degree. Because the cube corner is much more tolerant of angular misalignment than is the retro-telescope, it was chosen for use in absolute calibration of the instrument. This cube corner, which has a two-inch capture area, would be usable for absolute calibration out to one-half mile. Under optimum weather conditions, we were able to operate the system over the two-mile range with the same cube corner. The return from the cube corner was steady, almost scintillation-free, and repeatable from day to day. It was consequently judged adequate for calibration purposes.

The response of the ILAMS system to ethylene and ammonia in the gas cells was always the same, to the limit of our measuring ability. The response was linear with optical thickness (concentration times path length) and independent of the size of the cell. The 27-foot gas cell was calibrated against the 6-inch cell. Because they were both the same cross-section -- 6 inches inside diameter -- one milliliter of ethylene always produced the same result, (18% absorption — σ CL = 0.20) in either cell. Similarly, one milliliter of ammonia always produced 14% absorption (σ CL = 0.15). These results were independent of weather conditions, signal level returned, time of day, etc. These environmental factors influenced the system noise, but not its sensitivity nor its calibration.

Table X summarizes the data taken at the rural test site in Cazenovia, N. Y., during the last twenty-four hours of measurement. More than fifty hours of data were taken previously and are recorded. All charts are stored and indexed. All the data confirm the conclusions that may be drawn from this table. The data taken before March 18 were recorded on three small recorders -- two 2-channel brush recorders and one 2-channel Sanborn corder. Only six channels were available, and two of these were noisy because of recorder malfunction. No signal level channel was recorded on these data, so we had to depend upon operator comments to indicate low signal. Because of these facts, and also because of the other considerations explained under the section dealing with "measurement problems", the data taken after March 18 were considered to be the most accurate. The noise and drift data were read directly from 8-channel recorder chart records such as that shown in Figure 19. Because of the log amplifier, the meters read directly in terms of α CL. However, for such small values as those recorded here, one may multiply by one hundred and read them as percent absorption. Thus, an α CL of 0.04 may be read as a 4% absorption. The scintillation is the percent modulation as observed on the oscilloscope. The correlation between weather conditions and the observed scintillation bounce on the oscilloscope (Figure 20), presents no surprises. On two occasions, the scintillation did peak up again, around midnight, on a cold clear night with low wind. No ready explanation has been offered to explain this phenomenon. No such effect was noted during the urban testing. The correlation between the observed scintillation and the noise and drift errors as recorded on the strip charts (Figure 21), is also expected.

Where snow flurries are indicated on the data, one should not conclude that the sky was overcast. The winter weather in the lee of Lake Ontario often includes snow flurries together with clear sky, hazy sky, or scattered clouds. Thus, we were often faced with loss of signal due to a snow squall in the valley between the transmitter and the retroreflector while the sun was still shining.

Table X indicates that the noise and drift correlate very well. One may see, by looking at the chart record data, that the noise and drift are just the low- and high-frequency ends of a noise spectrum extending from dc to 0.2 Hz. The peak amplitude of the low-frequency noise, or dc drift, is not measurably different from the peak amplitude of the noise at the high-frequency end of the spectrum. Any lack of correlation between (1) the noise error and the drift error, or (2) between the scintillation as measured on the oscilloscope (Figure 21) and the noise and drift error, is attributable to the measurement inaccuracies -- that is, the accuracy with which we can measure noise from the oscilloscope and from the chart record.

TABLE X

LAST 24 HOURS OF DATA TAKEN AT RURAL TEST SITE IN CAZENOVIA, N. Y.

Run #	Temp °F	RH	Wind MPH	Scintillation % Modulation	Sky/ Precipitation	Noise (equivalent α CL)	Drift (equivalent α CL)	Period of Run
51	30-38°	60%	5-10	30%	clear	±0.04	±0.04	5:00 pm - 1:00 am
52	37°	37%	16	20%	hazy (flurries)	±0.02	±0.02	1:00 pm - 2:00 am
53	39-31°	55%	15	20%	hazy (flurries)	±0.03	±0.02	noon - 5:00 pm
54	39°	45%	5-10	40%	clear	±0.04	±0.05	3:00 pm - 4:00 pm
55	34°	50%	15-20	15%	flurries	±0.02	±0.03	1:30 - 4:30 pm
56	44°	31%	18-20	30%	clear	±0.02	±0.04	1:15 - 3:00 pm
57	61°	31%	8-15	10%	cloudy	±0.01	±0.01	2:50 - 3:30 pm
58	53°	36%	25-35	20%	scattered clouds	±0.02	±0.03	2:00 - 4:20 pm
59	41°	86%	12	10%	drizzle	±0.02	±0.02	2:25 - 3:30 pm
60	39°	96%	8-15	15%	light rain	±0.02	±0.03	2:10 - 4:35 pm

A

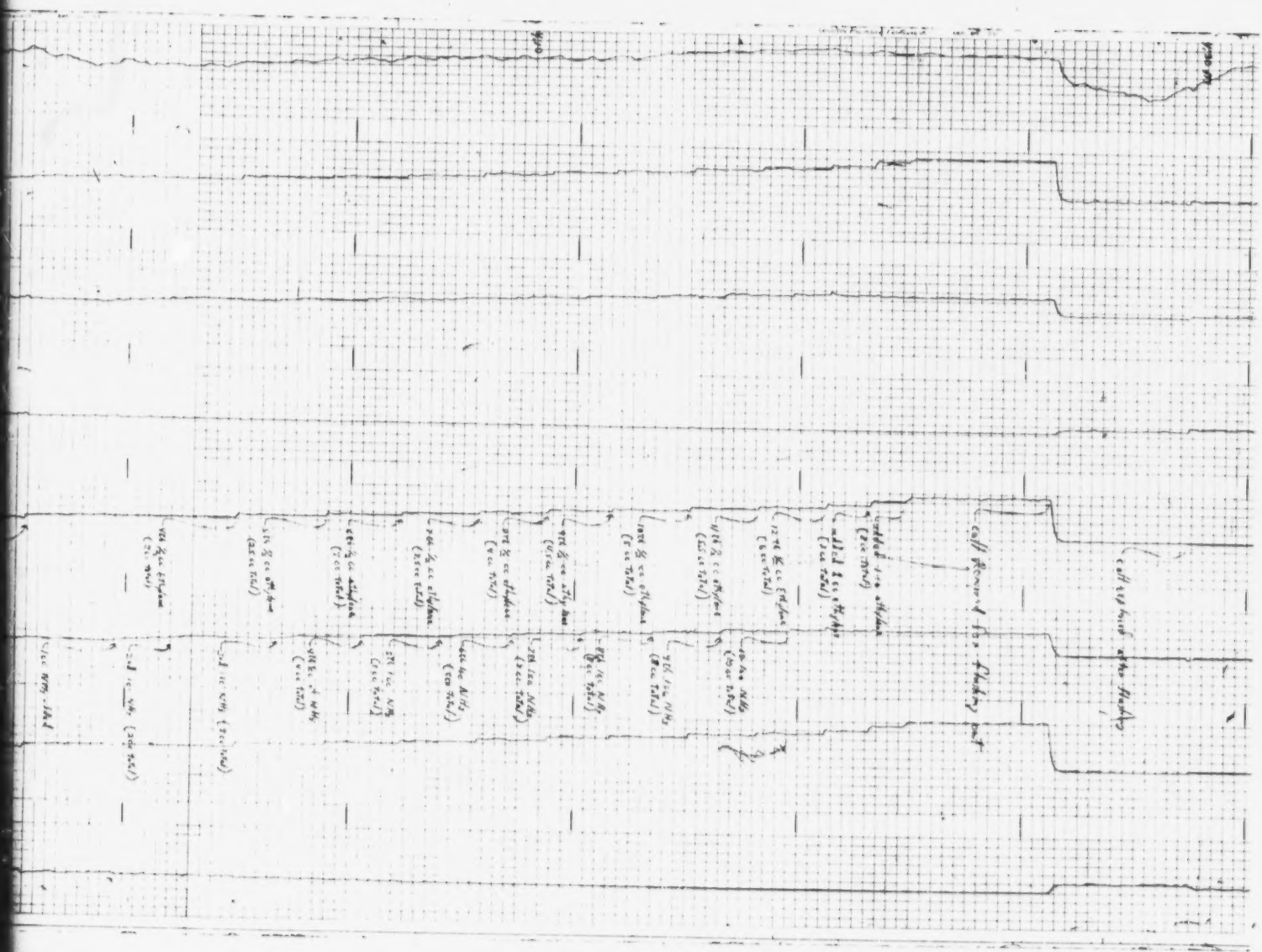

Figure 19. Chart Record

B

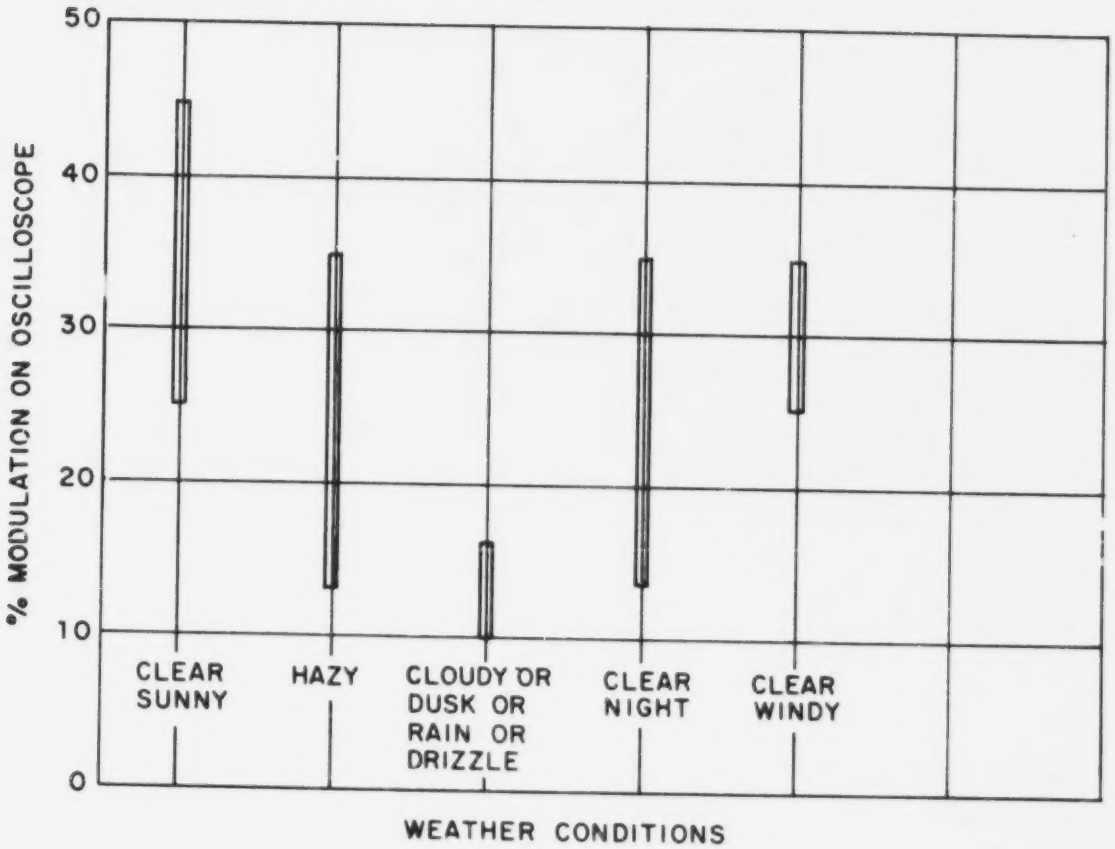

Figure 20. Relationship between Scintillation and Weather at Rural Site

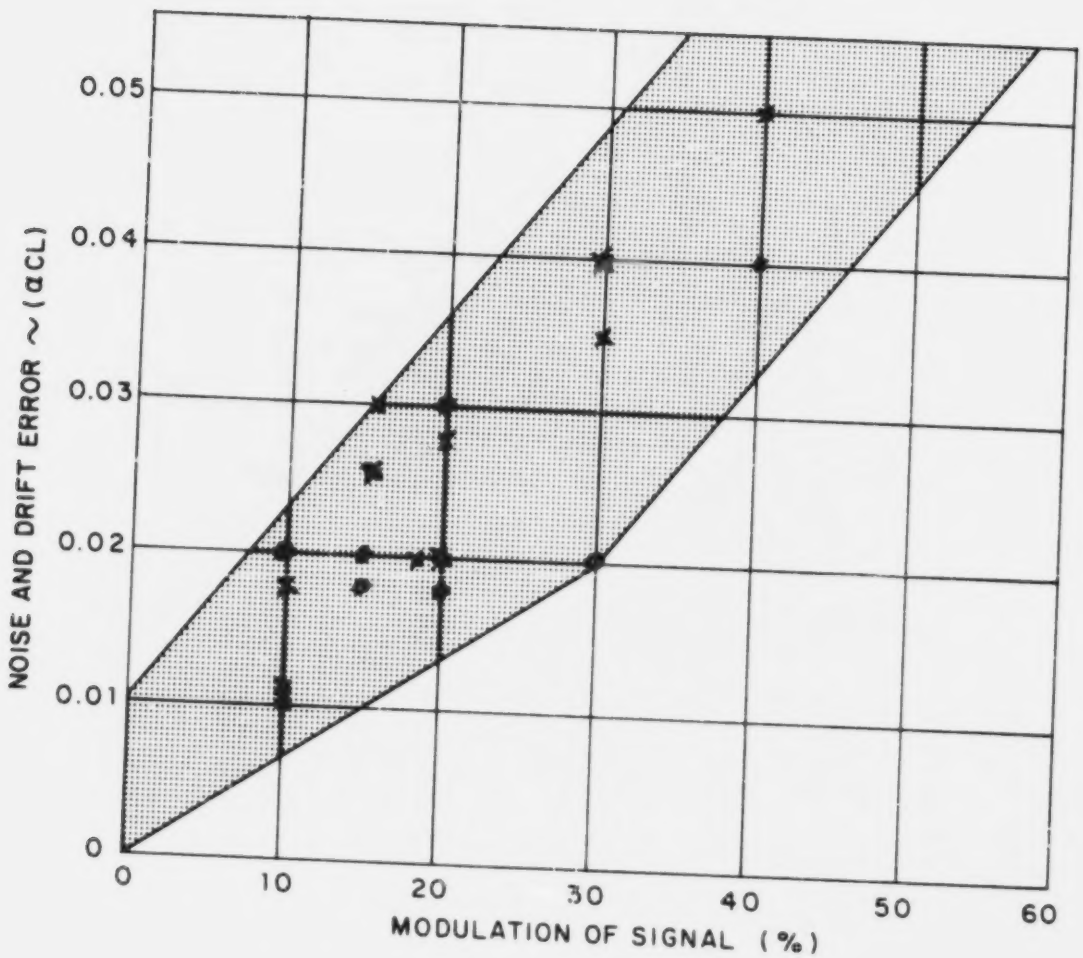

Figure 21. Relationship between Scintillation and Noise & Drift

VII. TRANSFER TO URBAN SITE

The selected urban site at Skytop is shown on the geological survey maps accompanying this report. Four locations were tried and two finally used; these are shown at the ends of lines radiating from the Skytop site. The seven-and-one-half-mile path between Skytop and General Electric's Electronics Laboratory proved to be too long for summertime operation. The attenuation due to water vapor alone should have been between 20 dB and 30 dB. (Refer back to Table V). A return signal was received from the retroreflector in clear but hazy weather, but only marginal operation was achieved. The reflector was then moved to the top of the Effluent and Chemical building at the Onondaga County sewage disposal plant on the southeast end of Onondaga Lake, which forms the northwest border of Syracuse. This reflector site was four-and-one-half miles from the laser system and the line between them runs over the center of the city. Although a large signal was received back from the retroreflector, the scintillation was also extremely large -- much larger than we expected. At the time, we thought that heating of the roof caused the scintillation. In the light of more recent data, it is now suspected that possibly a slight misalignment of the retrotelescope was the major cause of trouble. In mid-August, the retrotelescope was moved to the top of the State Office Building in central Syracuse, three miles from Skytop. Most of the data were taken over this range. The shorter two-mile range, also shown, will be discussed under Urban Measurements (Section VIII).

Skytop is a hill owned by the University of Syracuse, overlooking the City. Before transfer to Skytop, the ILAMS was installed in a sixteen-foot office trailer, along with the recording equipment. Then the system was aligned and tested over the rural range at Cazenovia. This proved to be a wise precaution. Severe instability problems with the new installation were caused by motion of the trailer. Efforts to stiffen the structure and support it on the ground with rigid supports failed. Wind loading and changes in the weight load of the trailer, such as people getting in and out and moving around inside, produced signifidantly large motions of the laser system. The effects of such motion will be discussed in Section IX. The trailer was mounted on three pedestals plus one large screw-jack adjusted so that the force on the four mounting points on the trailor's steel frame supported approximately equal weight. Mirrors were mounted at several points on the trailer, including on its steel frame, and angular motion of these mirrors was measured by the displacement of the reflected light from a small helium neon laser over a 70-foot path. No point could be found on the trailer frame or structure that did not move several milliradians as a 165-lb person walked about inside the trailer or got in and out of it. Mirrors mounted on the pedastals and on boards set between the pedestals showed that these points did not move. We concluded that the trailer could not be sufficiently rigidized to prevent flexing and distorting under these small load changes. This problem was solved by drilling 3" diameter holes through the trailer floor and building a steel frame through these clearance holes. At Skytop, a shallow pit was dug in the ground directly beneath the laser.

Approximately four inches of mixed sand and gravel were poured into the pit and concrete blocks were set on this bed. The laser sits on the steel frame and the frame sits on the concrete blocks. The steel frame is clear of the trailer floor, so that there is no mechanical connection between the laser and the trailer, except through the ground.

Figure 22a shows the nominal 16-foot office trailer in which we have installed our Laser Air Pollution Monitoring system. A large flat mirror is shown mounted on a tripod in front of the trailer, which serves to reflect sunlight into the remote retrotelescope for alignment purposes. Figure 22b shows the equipment installed inside the trailer. From left to right, we have the eight-channel Sanborn chart recorder, the four-wavelength signal processor, and the laser breadboard system mounted on sand-filled boxes that are supported above the floor from below the trailer. The photograph in Figure 22c shows the laser breadboard directed through the test cell and through the window to the retroreflector. Figure 22d shows the area of Syracuse, N. Y., being monitored. The retrotelescope is located in the center of the picture just above the tree line, three miles from the laser monitoring system. The tree line is approximately 1 1/4 miles distant.

a.

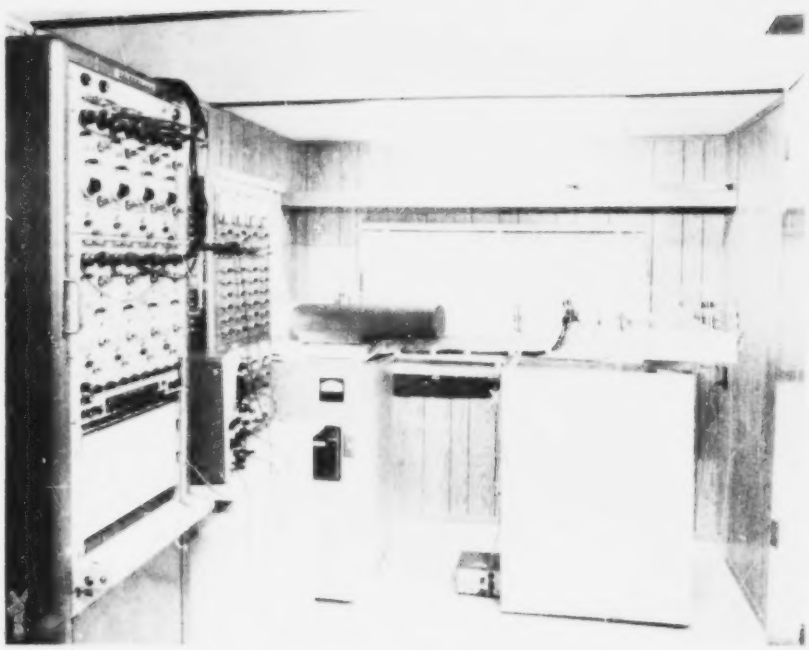

b.

Figure 22. Urban Test Site Photos (continued)

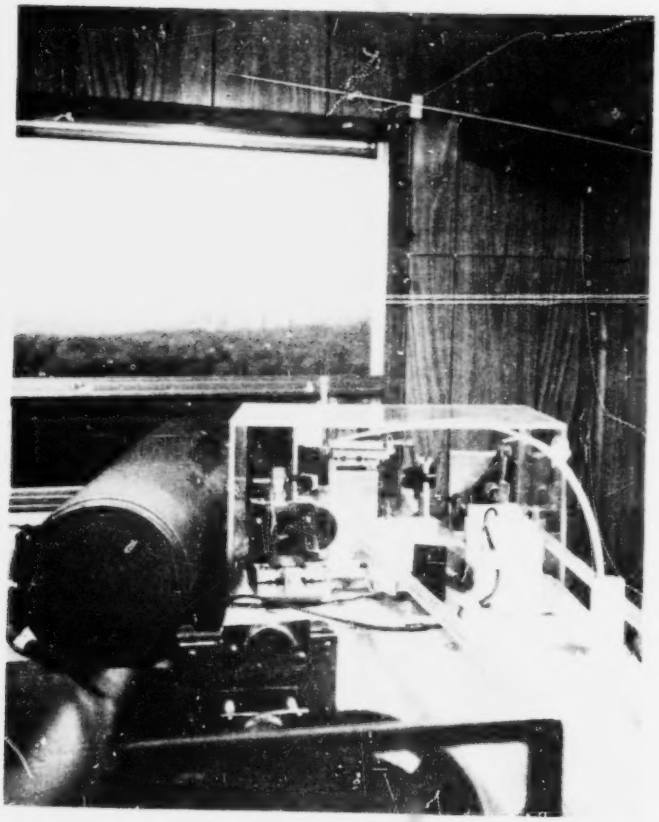

c.

d.

Figure 22. Urban Test Site Photos (concluded)

VIII. URBAN TEST SITE MEASUREMENTS PROGRAM

A. SUMMARY OF URBAN TEST RESULTS

Based on the excellent results with the test cells -- both the 27-foot cell and the 6-inch cell -- in measuring ammonia and ethylene, and the poor success in finding sufficient concentration of ethylene in Syracuse, the contract officers, Mr. John Nader and Dr. H. M. Barnes, recommended that we go ahead with the plans to monitor the air over Syracuse, N. Y., and use the test cells to measure system sensitivity. Injection of measured amounts of ethylene and ammonia gas into a 6-inch-long, 6-inch-diameter cell was used as the measure of the ILAMS sensitivity. As expected, the sensitivity of the system was the same as at the rural site.

More than twenty-four hours of data were recorded on chart paper over the period of August through December, 1971.

Noise and scintillation were slightly greater (approximately 30%) over the city than at the rural site. Drift was about the same on some days and unusually large on others. Whether this drift was caused by a spectral absorber like ethylene was not confirmed. This was the only departure in the behavior of the laser system from that at the rural site.

B. URBAN TEST RESULTS

The majority of the effort on this program was spent on the rural measurements program. It was felt that once the behavior of the system was well understood, system performance at the urban site would match that at the rural site. The emphasis in the urban measurements program was to look for differences in the behavior of the ILAMS, if any, in the urban as compared to the rural environment. The only difference noted was that the scintillation was larger with an attendant increase in the noise and drift error. This fact caused us to look more closely at the system, the monitored path, and the reflectors to isolate the causes of the measured scintillation noise and determine how much of it was inherent in the measuring technique.

The first retrotelescope site was the top of the Electronics Laboratory building on Electronics Parkway north of Syracuse. This site is approximately seven-and-one-half miles from the Skytop site, as may be seen on the enclosed topographical maps. The reflector used was the 12"-diameter Tinsley telescope, which is a Dall-Kirkham optical configuration with a 12" elliptical primary mirror, a 3" spherical secondary mirror located three feet in front of it, and has an effective focal length of 16 feet. The focal plane of the telescope is approximately four inches behind the hole in the primary mirror. A two-inch-diameter plane mirror was placed near the focal point on a sliding translation mount for focus adjustment. The focus was adjusted for peak signal using citizen-band walkie-talkies for communication between the Laboratory and Skytop. Sufficient return signal was received at Skytop for peaking, and

we believe that an optimum focus was achieved in spite of the marginal operation of the walkie-talkies at this distance. The signal return was, however, too small for good operation of the system. The combination of the high scintillation and poor atmospheric transmission regularly ran the signal level below 100 millivolts, causing large errors, as was discussed in Section VI. These measurements were made in July, when the absolute humidity was high and the power level return was pretty much as would be predicted from the extinction coefficients of Table V. The 7.5-mile test provided a good measurement of the range limit of the system.

The same telescope was used for the installation on top of the Chemical and Effluent building at 4.5 miles range. This site was discontinued because of excessive scintillation noise rather than weak signal. The reason for the very high scintillation noise was never discovered. With hindsight, we now believe that the retrotelescope was improperly focussed. At the time, it was not realized that this was a critical adjustment with regard to scintillation magnitude. Since the signal return was adequate, no attempt was made to improve the focus. In fact, it was speculated that perhaps deliberate defocussing of the return beam might improve scintillation, since slight defocussing of the transmitted signal did improve the scintillation noise at the Cazenovia site.

The Tinsley retrotelescope was moved, in mid-August, to the top of the State Office Building in Syracuse. All the recorded data, with the exception of run #110, were taken between this site and Skytop. The path length is 3 miles.

Very frequently, we had difficulty maintaining the retrotelescope in alignment and focus. Personnel working in the State Office Building would visit it and it would be found pointed in the wrong direction and/or out of focus. Although a great deal of time was lost in tracking down the source of weak signal return, one benefit did accrue. It was noted that the defocussed telescope often produced greatly magnified scintillation. A reexamination of the optics showed clearly that the secondary mirror, which obscures less than ten percent of the energy, produces a "shadow image" on the beam expander at the transceiver unless the plane mirror on the retrotelescope is set so that the return energy is focussed onto the beam expander. This focus point for the flat mirror is the plane of the real image of the beam expander in the telescope. With the flat mirror located at this point, the aperture of the beam expander is re-imaged back on itself by the retrotelescope. This focus is very critical. For example, if the plane mirror is moved 0.1 inches forward, then the return energy will exit via the retrotelescope collimated with a doughnut-shaped cross-section. This is the very condition we are trying to avoid.

A second retrotelescope reflector was mounted on a tripod, aligned, and calibrated against the reflector now mounted on top of the State Office Building in Syracuse. Calibration was accomplished by bringing the new reflector to the top of the state office building and taking data from the two telescopes separately and together. There was no spectral difference between the two reflectors, which was our main concern. The new telescope was then moved to the top of the Syracuse University mens' dormitory which lies almost exactly on a line with the transceiver on Skytop and the first reflector. The new reflector is just two miles from Skytop. This enabled us to obtain a

separate sampling of the first two miles and third mile. A second advantage of comparing the two-mile and three-mile systems is that they are optically identical.

During the calibration of the two telescopes against one another, the two were placed together -- one directly beneath the other -- and the transmit beam from the beam expander was defocussed slightly to accommodate both reflectors together. The result was no apparent increase in the return signal, but a large increase in scintillation, similar to the results we obtained at Cazenovia when using the cube-corner mosaic. A tentative explanation for this phenomenon is coherent interference between the two returns.

The second retrotelescope is a Criterion with a twelve-inch f/6 parabola for a primary mirror, with a two-inch-diameter 45 degree mirror mounted on a spider five feet in front of the primary. A one-inch-diameter flat mirror was used at the focus point to return the energy. The focussing tolerance must be better than 0.02 inches with this telescope at two miles, as compared to 0.1 inches with the Tinsley at three miles range. Similar scintillation problems were experienced with the focus of the Criterion retrotelescope, in spite of the fact that the obscuring secondary mirror is only 2 inches in diameter.

A single cube corner, masked down to 1/4 inch aperture, was mounted on a 14-foot mast, 150 feet in front of the laser transceiver, for calibration purposes and also to measure performance with a very nearby target. In terms of angle, the cube corner was halfway between the Criterion telescope on top of the mens' dormatory and the Tinsley on the State Office Building. The cube corner proved to be an extremely stable reference. No measurable scintillation or drift occurred using this nearby reflector. However, the optics of the system, using the nearby cube corner as a retroreflector, are different from the optics with the retrotelescope in two important ways. The output beam from the beam expander is normally focussed at a point halfway between the retrotelescope and the transceiver. Since the diameter of the retrotelescope is 2.5 times the exit aperture of the beam expander, the beam still does not overfill the retrotelescope. Minimum scintillation was observed at the rural site for this focus. Because the beam expander is so much larger than the cube corner, we cannot use the cube corner to simulate this condition. Secondly, in order to focus the energy from the beam expander at a point between the beam expander and the cube corner, it is necessary to back off the germanium focussing lens approximately $\frac{1}{2}$ inch. Since the germanium lens is operated off-axis in order to prevent reflections from the lens surfaces getting back to the detector, backing off the lens changes the centering of the output beam on the beam expander. This change in centering introduced the type of masking error described in Section VI. C.

Table XI is a summary of the urban test site data recorded on chart-recorder paper. The charts are indexed according to the run numbers. All these measurement runs were made between Skytop and the State Office Building, with the exception of run #110, which was made between Skytop and the mens' dormatory. Figure 23 shows the relationship between the scintillation and weather. Figure 24 shows the noise and drift error versus scintillation magnitude. Because of the large variance in the data, we do not feel that the differences between these results and the rural results are very significant. One major difference that does not show on Table XI, nor on the figures, is

TABLE XI. URBAN TEST SITE DATA

Run #	Temperature °F	RH	Wind MPH	Scintillation % Modulation	Sky	Precipitation	Noise (equivalent α CL)	Drift (equivalent α CL)	Period at Run
101	63°	50%	10-15	25%	Hazy	Zero	±0.02	±0.02	3:20-4:00 pm
102	70°	40%	5	45%	Few Clouds	Zero	±0.05	±0.04	2:00-3:30 pm
103	87°-74°	70%	5-10	25%	Cloudy	Zero	±0.04	±0.04	3:30-11:00 pm
104	75°	60%	8	40%	Clear	Zero	±0.04	±0.04	4:00-4:50 pm
105	65°-70°	75%	0-5	30%	Clear	Zero	—	±0.06	9:50 am-12:30
106	70°	55%	10-15	20%	Hazy	Zero	±0.02	±0.04	11:00 am-1:00 pm
107	60°	90%	10-15	15%	Cloudy	Light Rain	±0.02	±0.04	10:00 am-2:00 pm
108	50°-40°	60%	5-10	35%	Clear	Zero	±0.04	±0.07	4:10-4:00 pm
109	35°-30°	60%	10	15%	Cloudy	Snow Showers	±0.02	±0.03	1:15-4:15 pm
110	30°	85%	15	20%	Cloudy	Light Snow	±0.03	±0.03	1:00-5:00 pm
111	45°	60%	15-20	25%	Cloudy	Zero	±0.02	±0.04	11:00-noon
112	39°	76%	10-15	35%	Cloudy	Drizzle	±0.04	±0.03	3:30-4:45 pm
113	35°	40%	10	45%	Cloudy	None	±0.06	±0.03	2:50-3:30 pm

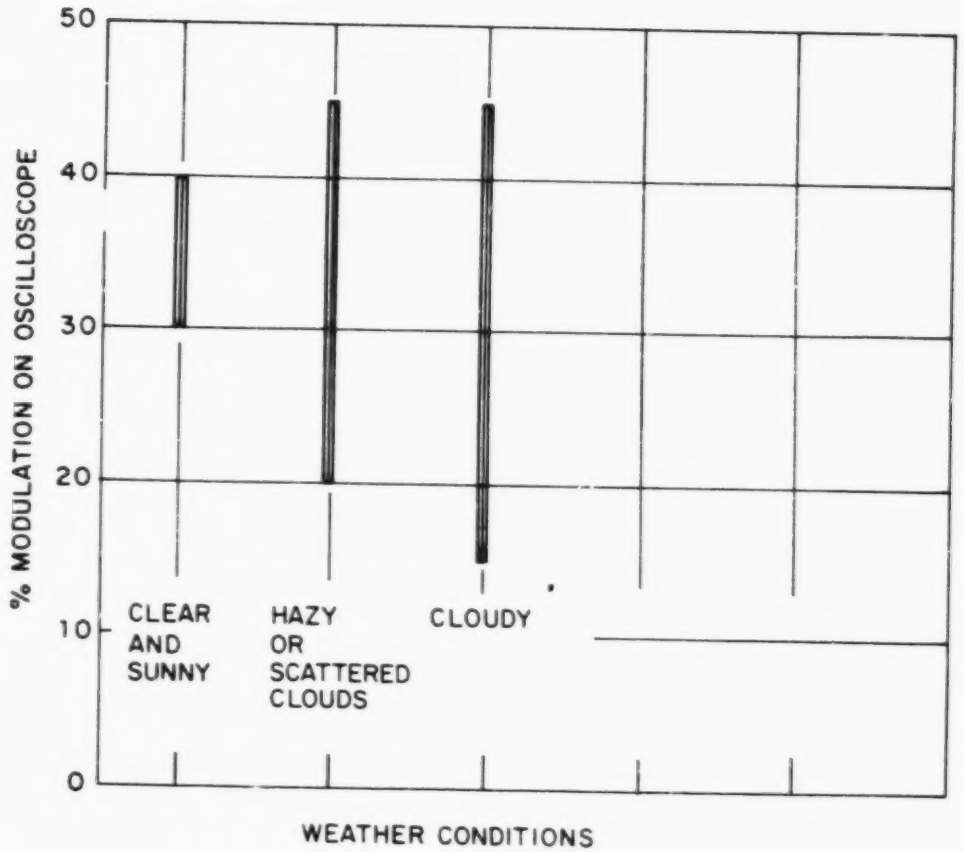

Figure 23. Relationship Between Scintillation and Weather at Urban Site (Skytop)

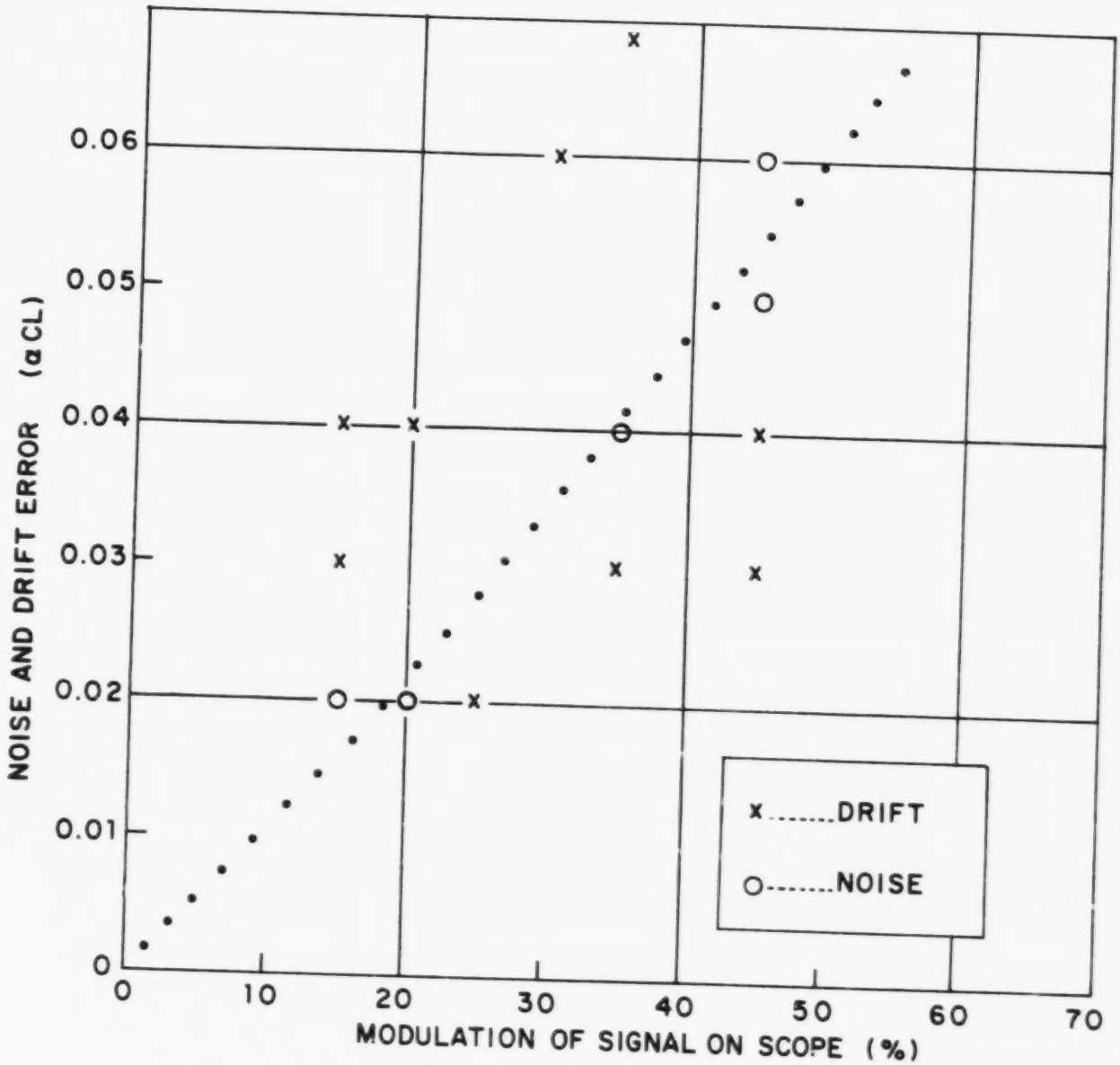

Figure 24. Relationship Between Scintillation and Noise & Drift (Urban Site)

that, on a few of the runs recorded (and several times not recorded on chart paper), an apparent ethylene absorption came and went over a period of an hour or two. This was either a local spectral absorption, or else a system error. Neither hypothesis has been confirmed. The absorption signals measured corresponded to αCL of from 0.1 to 0.25. This would require an average concentration of ethylene of from 13 ppb to 32 ppb over one mile, or an average concentration of from 675 ppb to 1,700 ppb, spread over 100 feet. We found no indications of such concentrations in open areas in Syracuse.

C. SYSTEM IMPROVEMENT WITH A CLEANUP APERTURE

As was pointed out in Section VI., the lack of similarity in the spatial power distribution of the exit beams at the four wavelengths, as shown in Figure 18, is the main source of error in the ILAMS. The conventional solution to this problem is to introduce a spatial filter in the form of a very small circular aperture (pinhole) at a focus point of the beam before it is transmitted. Unfortunately, the design of this laser system is such that the introduction of such an aperture is not easy without some modification of the external optics. The focus point of the germanium lens immediately preceeding the beam expander will not suffice for this purpose, for three reasons. First, a large percentage of the energy rejected by the aperture will be reflected directly back to the signal detector as a false signal return; secondly, any variation in the transmitted energy through the aperture caused by laser beam wander will not be compensated for by the reference detector; and thirdly, if it is desired to defocus the transmit beam slightly, then the return signal from the retrotelescope will not focus at the same point as the aperture and considerable energy would be wasted. In clear weather over moderate ranges, this last consideration is not as important.

The ideal location for the spatial filter is between the coupling mirror and the beam splitter. If a pair of small, short-focal-length lenses could be mounted back to back in a confocal configuration in the small space available, then the pinhole could be placed at the common focal point of the two. If such an aperture is smaller than two wavelengths in diameter, or smaller than the diffraction pattern of an ideal laser beam at the focus of the lens, then it will clean up or filter out any spatial variations in the pattern in both the near field and the far field, except for variations in size. The variations in size would occur because the diameter of the far-field diffraction pattern is proportional to wavelength. The size variation would be a source of error if the output from the beam expander were focussed on the retrotelescope. Then the beam patterns for different wavelengths at the telescope would be concentric and similar, but of different sizes. Thus, if the beam moved, an unbalanced or false absorption would be produced. This error can be reduced by defocussing the transmit beam from the beam expander, so that angular displacements of the beam caused by atmospheric turbulence would not easily result in percentage changes in reflected return that are different from wavelength to wavelength. The focussing of the energy return from the retroreflector presents the same problem. One might argue that, because light travels the round trip to the reflector and back in a short time compared with the speed of atmospheric changes, if the energy found its way to the reflector by some crooked path, then it would follow the same path back and there would be no scintillation effects interfering with the return trip. The fact is that thermal gradients in the vicinity of the retrotelescope would cause the return beam to

wander, because the energy enters and exits on opposite sides of the telescope. This effect has been confirmed by experiment. The conflict between the need for focussed return from retrotelescopes with obscuring secondary mirrors and the need for defocussed return to eliminate scintillation effects because of the different size of the focussed beams at each wavelength may be resolved by using another type of telescope as a retroreflector. Either an off-axis parabola like the beam expander, or a telescope with a very small secondary mirror would make good retrotelescopes.

The modifications needed to test the spatial filter approach properly were deemed too extensive to undertake during this project. However, a compromise was attempted as shown in Figure 25. Two apertures, 0.044-inch-diameter and 0.081-inch-diameter, were tried between the coupling mirror and the beam splitter without the addition of any focussing optics. This approach had the disadvantage that a great deal of energy was thrown away in order to get a small enough aperture to get some spatial filtering. It was not known whether any improvement at all would be realized, because some spatial zoning could still occur within the aperture. To be effective, the spatial filter or aperture must look like a point source. That is, the aperture must be small enough so that the transmit optics cannot resolve the difference between it and a true point source of power. The apertures we used were as small as could be tolerated and still have a sufficient signal return. If it had been possible to install the focussing lenses suggested above, we could have used a sufficiently small aperture with only 75% loss in power.

The results of the test were very encouraging. The reduction in scintillation noise was approximately three to one. The reduction in drift was four to one and, for the first time, we seemed to have close to an absolute calibration. Absolute calibration means that the relative power returned from wavelength to wavelength is the same as the relative power from wavelength to wavelength seen by the reference detector. There was no need to correct for any fixed absorption pattern related to the transmit receive optics, because such an absorption pattern was reduced by approximately ten to one. It is suspected that the remaining drift and spectral scintillation noise was related to the focussed beam size differences plus the remaining spectral zoning.

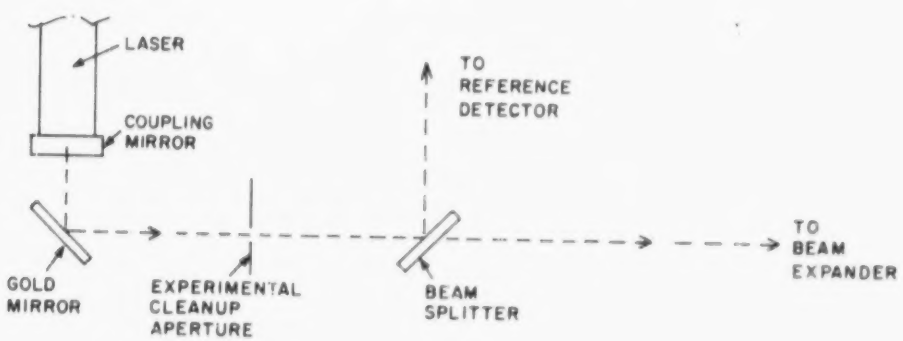

Figure 25. Location of Cleanup Aperture

IX. SUMMARY OF SYSTEM PERFORMANCE EVALUATION

Several sources of error in making measurements were identified during the course of the measurements program. These problems and their resolution are outlined here.

1. Severe Scintillation Induced by Local Heat Sources

Heat loading from direct and reflected sunlight on the test cell, room heat on the polyethylene windows separating the test cell from the room, sun loading on the west wall of the building housing the retroreflector, cold air from the polyethylene window in and near the beam expander, and at one point heating tape near the retroreflector – these factors were all sources of scintillation producing thermal gradients. The thermal problems were partially solved by the use of sun shielding on the retroreflector building and the test cell, and multiple-layer polyethylene windows at the room-air to outside-air interface. The scintillation associated with the twenty-seven-foot test cell was never completely eliminated until the cell was removed.

2. Long Term Unbalance or Drift Error Produced by Changing the Attitude or Pointing Direction of the Laser Transceiver and then Correcting for this by Translating the Germanium Focusing Lens at the Entrance to the Beam Expander

This correction moves the beam slightly in the exit aperture. Because of the asymmetry of the transmitted wavelengths (see Figure 18), this translation of the beams on the beam expander mirror produces a change in the masking by the mirror and a resultant signal unbalance. The cause of this motion of the laser system was a mystery for some time, until it was discovered that the floor was heaving from ice formation under the building edges and under the unheated portions of the building. As spring came, this problem solved itself. Accidental bumping of the laser system, which pushed it out of alignment, would of course produce the same result unless it was corrected by moving the laser itself rather than the germanium lens.

3. Unbalance Caused by Aiming Error from Transmitter to Retroreflector

If a misalignment such as described in (2.) occurred, and was not corrected for, by either moving the germanium or moving the laser, then a more serious unbalance or drift error occurred. The lack of similarity of the different wavelengths shown in Figure 18 has a corresponding lack of similarity and concentricity in the far field at the retroreflector. If the laser output beam wanders with respect to the support frame, then any error so caused will be compensated for by the reference aperture, because this aperture sees the same portion of far field pattern as the retroreflector does. But if the aiming error is caused by motion of the ILAMS frame structure, or by displacement of the beam on the

retroreflector by scintillation (thermal gradients in the air), then a wavelength-to-wavelength unbalance or drift error occurs. The magnitude of this error is much larger than the masking error we get if we correct by translating the germanium lens. During the rural measurements, no solution for this problem was found. The drift error caused by scintillation in this way was judged to be the dominant source of noise and drift error in the system.

4. Direct Coupled Amplifier Drift and Paper Slippage in the Chart Recorders

The meters on the signal processor permitted observation of both the synchronous detector outputs at each wavelength and the weighted outputs. It was noted that, often after many minutes of running time, the chart recorder outputs did not correspond to the meters. There were two causes for this discrepancy: (1) the chart paper would slip sideways slowly on the rollers so that all channels would appear to drift off together and (2) the dc amplifiers in the chart recorder would drift so that their output voltage would change for zero change in input voltage. Both of these effects produced pseudo-errors of more than 10% absorption (α CL = 0.1) at times. Checks on the recorder drift were made by disconnecting the output from the signal preamplifier and then connecting the reference preamplifier to both AGC inputs. This produced zero output on all channels with no drift. After checking the recorder drift, the operator would measure the false error, make the correction and note it on the chart paper.

5. Errors Caused by System Noise

System noise had no effect upon the ILAMS performance, except under the following conditions. When the total effect of (a) poor transmission in the atmosphere, (b) absorption by a specific gas, (c) loss by the sample cell windows, plus (d) any instantaneous drop in signal caused by scintillation, caused any of the four wavelengths to drop in power level to the point were the preamplifier output voltage was 100 millivolts or less, then the system noise caused the log amplifier to see a negative voltage resulting in such large output errors from the log amplifier that the system was considered inoperable. Over the two-mile range in clear weather, with no test cell in the path, approximately 500 times this signal level was available. Six-inch circles of copper window screen were used as neutral attenuators, so that we could work with such large signal return without overdriving the preamplifiers. The result was that, by using these attenuators and removing them as the available signal dropped, an attenuation of up to 500:1 (including scintillation) could be tolerated.

6. Unusually Large Scintillation Caused by Defocusing the Retrotelescope

Unless the retrotelescope is properly focused (not aimed), the shadow of the partially obscuring secondary mirror on the telescope is imaged back on the beam expander aperture of the ILAMS. Hence, the transceiver would receive no return energy except when scintillation was present. This sort of alignment tended to maximize scintillation, producing 100% modulation of the signal return. The problem did not arise at the rural site, because the retrotelescope was in a

well-protected environment and because there was an excellent communications link between the two sides of the valley for use in alignment and focusing. Defocusing of the retroreflector was a constant problem in the urban tests because of some combination of wind and peoples' curiosity. The problem was solved simply by realigning whenever the retrotelescope appeared to be out of focus. The ultimate solution will be to provide better protection for retroreflectors.

7. Detection of 14 ppb Ethylene, 19 ppb Ammonia

The system sensitivity under the worst conditions of scintillation and drift was never worse than an α CL of 0.1. That is, we could always reliably detect an absorption of 10% at one wavelength compared to the others. The resultant sensitivity to ethylene over the two-mile path was 14 ppb and to ammonia 19 ppb.

8. Projected Performance Capability

With a cleanup aperture added to the ILAMS, the expected sensitivity is from an α CL of 0.01 to 0.001, which should greatly extend the usefulness of the system in measuring trace constituents in the atmosphere, even over short ranges.

REFERENCES

1. Philip L. Hanst, Private Communication, 1970

2. Yates and Taylor, NRL Report 5453, 1960

3. A. R. Curtis and R. M. Goody, "Spectral Line Shape and Its Effect On Atmospheric Transmission," Quart. J. Roy. Meteorol. Soc., Vol. 80, p. 58 (1954).

4. Migeotte, M., Neven, L., and Swensson, J., "The Solar Spectrum From 2.8 to 23.7 Microns, Part 1, Photometric Atlas," Technical Final Report, Phase A, Part 1, Contract AF61(514)-432 (1957).

5. "Water Vapor Continuum Absorption of Carbon Dioxide Laser Radiation Near 10μ", John H. McCoy, David B. Rensh and Ronald Long; July 1969, Vol. 8, No. 7; Applied Optics, p. 1473.